USGS
science for a changing world

Eruption Probabilities for the Lassen Volcanic Center and Regional Volcanism, Northern California, and Probabilities for Large Explosive Eruptions in the Cascade Range

Scientific Investigations Report 2012–5176–B

U.S. Department of the Interior
U.S. Geological Survey

Eruption Probabilities for the Lassen Volcanic Center and Regional Volcanism, Northern California, and Probabilities for Large Explosive Eruptions in the Cascade Range

By Manuel Nathenson, Michael A. Clynne, and L.J. Patrick Muffler

Scientific Investigations Report 2012–5176-B

U.S. Department of the Interior
U.S. Geological Survey

U.S. Department of the Interior
KEN SALAZAR, Secretary

U.S. Geological Survey
Marcia K. McNutt, Director

U.S. Geological Survey, Reston, Virginia: 2012

For product and ordering information:
World Wide Web: http://www.usgs.gov/pubprod
Telephone: 1-888-ASK-USGS

For more information on the USGS—the Federal source for science about the Earth,
its natural and living resources, natural hazards, and the environment:
World Wide Web: http://www.usgs.gov
Telephone: 1-888-ASK-USGS

This report and any updates to it are available online at: http://pubs.usgs.gov/sir/2012/5176/b/

Suggested citation:
Nathenson, M., Clynne, M.A, and Muffler, L.J.P., 2012, Eruption probabilities for the Lassen Volcanic Center and regional volcanism, northern California, and probabilities for large explosive eruptions in the Cascade Range: U.S. Geological Survey Scientific Investigations Report 2012-5176-B, 23 p. (Available at http://pubs.usgs.gov/sir/2012/5176/b/)

Contents

Figures

Tables

Eruption Probabilities for the Lassen Volcanic Center and Regional Volcanism, Northern California, and Probabilities for Large Explosive Eruptions in the Cascade Range

By Manuel Nathenson, Michael A. Clynne, and L.J. Patrick Muffler

Abstract

Chronologies for eruptive activity of the Lassen Volcanic Center and for eruptions from the regional mafic vents in the surrounding area of the Lassen segment of the Cascade Range are here used to estimate probabilities of future eruptions. For the regional mafic volcanism, the ages of many vents are known only within broad ranges, and two models are developed that should bracket the actual eruptive ages. These chronologies are used with exponential, Weibull, and mixed-exponential probability distributions to match the data for time intervals between eruptions. For the Lassen Volcanic Center, the probability of an eruption in the next year is 1.4×10^{-4} for the exponential distribution and 2.3×10^{-4} for the mixed exponential distribution. For the regional mafic vents, the exponential distribution gives a probability of an eruption in the next year of 6.5×10^{-4}, but the mixed exponential distribution indicates that the current probability, 12,000 years after the last event, could be significantly lower. For the exponential distribution, the highest probability is for an eruption from a regional mafic vent. Data on areas and volumes of lava flows and domes of the Lassen Volcanic Center and of eruptions from the regional mafic vents provide constraints on the probable sizes of future eruptions. Probabilities of lava-flow coverage are similar for the Lassen Volcanic Center and for regional mafic vents, whereas the probable eruptive volumes for the mafic vents are generally smaller.

Data have been compiled for large explosive eruptions ($>\approx 5$ km^3 in deposit volume) in the Cascade Range during the past 1.2 m.y. in order to estimate probabilities of eruption. For erupted volumes $>\approx5$ km^3, the rate of occurrence since 13.6 ka is much higher than for the entire period, and we use these data to calculate the annual probability of a large eruption at 4.6×10^{-4}. For erupted volumes ≥10 km^3, the rate of occurrence has been reasonably constant from 630 ka to the present, giving more confidence in the estimate, and we use those data to calculate the annual probability of a large eruption in the next year at 1.4×10^{-5}.

Introduction

The Lassen Volcanic Center and its predecessors are distinguished from the surrounding regional mafic volcanism in northern California by their greater longevity, larger volumes, and broader range of silica concentrations (Clynne and Muffler, 2010). Clynne and others (2012) provide chronologies for eruptive activity at the Lassen Volcanic Center and for eruptions from the regional mafic vents in the surrounding area of the Lassen segment of the Cascade Range for the past 100,000 years (for geographic extent covered, see Clynne and others, 2012, fig. 4). We use these chronologies to calculate probabilities of future eruptions. Areas and volumes of lava flows and domes have been estimated on the basis of geologic mapping (Clynne and Muffler, 2010; M.A. Clynne and L.J.P. Muffler, written commun., 2010), and these values are presented in time histories and used to calculate probabilities of sizes of eruptions.

An underlying assumption of past U.S. Geological Survey (USGS) volcano hazards assessments for Cascade Range volcanoes in Oregon and Washington has been that the probability distribution of time intervals between volcanic eruptions may be treated as a Poisson process. Recent works on USGS hazard assessments, however, have applied other probability distributions to calculating the probability of an eruption in the next year based on the time since the last eruption (Christiansen and others, 2007; Nathenson and others, 2007). These new works use the matching of time histories containing disparate time intervals between eruptions, with a few intervals being much longer than most of the time intervals. The Lassen chronologies are used in this report with several probability distributions to check if the estimates are better than those using a Poisson process. The probabilities thus obtained provided a basis for assessing the volcanic hazards in the Lassen area in Clynne and others (2012).

The eruptions documented for the past 100,000 years in the Lassen segment of the Cascade arc do not represent the full spectrum of possible eruptions, because no large explosive eruptions have occurred during this period. Before 100 ka, however, the Lassen segment of the Cascade arc has been the site of several large explosive eruptions during the past

few million years. Instead of calculating the probability of a large explosive eruption in the Lassen area, we shall instead calculate probabilities of large explosive eruptions for the Cascade arc as a whole. To do this, data for the past 1.2 m.y. have been compiled and analyzed.

Chronologies

The chronology of eruptive events at the Lassen Volcanic Center during the past 100,000 years is given in table 1 (also given in Clynne and others, 2012). This time period was chosen in order to have enough events for analysis but to stay within the more recent history of the Lassen Volcanic Center. No activity is known to have occurred in the Lassen Volcanic Center between 190 ka and 90 ka (Clynne and Muffler, 2010), and that long hiatus indicates a likely resetting of the magmatic system. Even if there were small eruptions during this period that are missing from the geologic record, the lack of larger eruptions still indicates that there has probably been a change in the magmatic system. Activity during the past 100,000 years is divided into the Eagle Peak and Twin Lakes sequences (table 1). The division is based primarily on the Eagle Peak sequence being more silica rich (dacite and rhyodacite) and the Twin Lakes sequence being less so (basaltic andesite and andesite). The Eagle Peak sequence consists of seven units of domes and flows and their pyroclastic deposits and includes the prominent young features of Lassen Peak and Chaos Crags. The Twin Lakes sequence comprises lava flows and cones and includes the youngest eruptions—the 1914–17 eruption of Lassen Peak and the 1666 C.E. basaltic andesite of Cinder Cone. The time history of event occurrence for the Lassen Volcanic Center (fig. 1) shows an approximately constant rate. The three most recent events occurred at a faster rate, but similar behavior also occurred about 40,000 years ago. Areas and volumes of lava flows are given in table 1, and the additional areas and volumes of fragmental deposits are given in the notes column. The time history of cumulative area and volume of lava flows (fig. 2) is more variable in rate than that for event occurrence.

The chronology of eruptions from regional mafic vents for the past 100,000 years in the surrounding area of the Lassen segment of the Cascade Range is given in table 2 (also given in Clynne and others, 2012). The events have been grouped into eruptive sequences, with the remainder not falling into a sequence placed in a miscellaneous group. The eruptive sequence groupings for the mafic vents are based on a combination of geographic locality and petrographic characteristics of the eruptive products. Mafic magmas cannot spend much time in the crust without significant evolution of their petrography. Thus the similarity of petrographic characteristics allows the various eruptions to be grouped as a sequence that must have been erupted over a relatively short amount of time. The Red Cinder chain, the Bidwell Spring chain, and the basaltic andesite of Turnaround Lake in the Tuya Chain (listed in the miscellaneous group, table 2) are the expression during this time period of the Caribou Volcanic Field east of the Lassen Volcanic Center (Clynne and Muffler, 2010). The Caribou Volcanic Field is an area of intense regional volcanism having a higher flux of basalt from the mantle compared to the rest of the regional volcanism, but not as high as that feeding the Lassen Volcanic Center (Guffanti and others, 1996).

Ages of many of the eruptions from regional mafic vents are known only within broad ranges, and we apply two models to make estimates of the ages of individual eruptions. The first model (model I) assumes that events occur evenly distributed within the given age range for a sequence. Chosen ages for each sequence were combined for the entire history, sorted, and then modified slightly so that no two events in the entire history had the same age. The second model (model II) assumes that events within a given age range occur closely spaced in time near the event with a measured age. This close spacing in time may be a more realistic model, compatible with the similar petrography within each eruptive sequence. Again, chosen ages for each sequence were combined for the entire history, sorted, and then modified slightly so that no two events in the entire history had the same age. Except for the two events near Sifford Mountain, the events in the miscellaneous group are not likely to be related to other events, and their ages in both models are the same.

The chronologies for the eruptive sequences in the two models are shown in figure 3. The second model generally makes the eruptive sequences become more a series of episodes than a series of events. For example, the Red Cinder sequence changes from a series of events over a long time period to three episodes of multiple events. The combined chronology of all the mafic vents is shown in figure 4. The order in which events occur in the combined chronology is not the same in the two models. Grouping the ages near measured ages in the individual sequences (model II) also results in an episodic character to the combined eruptive history, whereas the results for the first model are only somewhat episodic. The most recent of the regional mafic eruptions were two events with estimated ages of 15–10 ka. The second model has one hiatus of 14,000 years and four in the range of 5,000 to 7,000 years, whereas the first model has only three hiatuses in the range of 5,000 to 7,000 years. This difference in the number of long-term hiatuses between the models makes the current hiatus of 10,000 to15,000 years not appear to be such a special time with the second model. Given the broad spread in age ranges for each sequence, the true chronology could be different from either model, but for purposes of calculating probability distributions of times between eruptions, the modifications should not make a large difference. Because the total time is constant, every interval that is shortened lengthens an adjacent interval. The rate of occurrence of events for model I appears somewhat higher since 50 ka. For model II, the earlier and later periods show similar rates of occurrence separated by intervals of no events or a lower rate of events. Plots of cumulative area (fig. 5) and cumulative volume (fig. 6) have similar patterns of rates. There does appear to be an increase in rates of volume produced and areal coverage

Table 1. Chronology of eruptions less than 100,000 years old in the Lassen Volcanic Center.

[Data from Clynne and others (2012) and Clynne and Muffler (2010); recent eruptions from historical record. Ages with uncertainties are measured using $^{40}Ar/^{39}Ar$, K-Ar, or radiocarbon. Others are estimates constrained by stratigraphy and geomorphology. Radiocarbon age is for weighted mean with standard error and is converted to calibrated age by choosing oldest peak based on paleomagnetic data (Nathenson and others, 2007). Age of andesite of Eagle Peak is chosen to be slightly younger than rhyodacite of Eagle Peak, as the waning stage of that eruption. Ages have been put on a common basis of years BP (before present), where present is 1950 C.E. Areas are calculated from mapped areas of lava flows, and volumes include additions for any associated domes. For parts of lava flows buried by surficial deposits, areas and thicknesses have been estimated, and they are added to the area and volume figures. Estimates of areas and volumes of fragmental deposit are provided in the notes column. The tabulation of volumes in Clynne and others (2012) includes most of the fragmental deposit volumes in the listed volume and differs from this compilation where volumes in the column are for lava flows.]

Eruption	Sequence	Age	Best age	Best age (years BP)	Area (km^2)	Volume (km^3)	Notes
Deposits of 1914–1917 eruption of Lassen Peak	Twin Lakes	1914–1917 C.E.	1914 C.E.	36	0.107	0.007	Volume is proximal juvenile component; additional volume of nonjuvenile material in debris flows not included. Lahars and pyroclastic flows cover an additional ~8 km^2. Distal tephra volume ~0.02 km^3.
Basaltic andesites of Cinder Cone	Twin Lakes	1666 C.E.	1666 C.E.	284	8.4	0.332	Tephra covers a minimum of an additional 96 km^2 area and 0.034 km^3 volume.
Rhyodacite of Chaos Crags	Eagle Peak	1,103±13 ^{14}C years BP	1,050 cal. years BP	1,050	4.54	1.00	Pyroclastic flow deposits cover a minimum of an additional 9.4 km^2 area and 0.15 km^3 volume. Airfall of 0.035 km^3 volume.
Andesite of hill 7416	Twin Lakes	~12–15 ka	13 ka	13,000	8.0	0.206	
Dacite of Lassen Peak	Eagle Peak	27±1 ka	27 ka	27,000	9.4	1.92	Estimate of pre-glacial area; pyroclastic flow deposits cover an additional 3 km^2 area and 0.15 km^3 volume.
Rhyodacite of Kings Creek	Eagle Peak	35±1 ka	35 ka	35,000	6.4	0.448	Includes 0.75 km^2 of buried lava; pyroclastic flow deposits cover an additional 8 km^2 area and 0.08 km^3 volume.
Andesite of Hat Mountain	Twin Lakes	~40 ka	40 ka	40,000	39.6	4.72	Includes 1.9 km^2 of buried lava flow.
Rhyodacite of Sunflower Flat	Eagle Peak	41±1 ka	41 ka	41,000	5.5	0.73	Includes 0.76 km^2 of buried lava; pyroclastic flow deposits cover an additional 2.35 km^2 area and 0.024 km^3 volume.
Rhyodacite of Krummholz	Eagle Peak	43±2 ka	43 ka	43,000	1.00	0.060	Includes 0.78 km^2 of buried lava flow.
Rhyodacite of Section 27	Eagle Peak	~50 ka	50 ka	50,000	0.75	0.0451	Includes 0.72 km^2 of buried lava flow.
Andesite of Eagle Peak	Twin Lakes	~66ka	65.9 ka	65,900	0	0	No lava flow; pyroclastic flow deposits cover 0.0201 km^2 area and 0.00060 km^3 volume.
Rhyodacite of Eagle Peak	Eagle Peak	66±4 ka	66 ka	66,000	1.14	0.074	Includes 0.12 km^2 of buried lava flow; pyroclastic flow deposits cover an additional 5 km^2 area and 0.015 km^3 volume.
Basaltic andesite of Fairfield Peak	Twin Lakes	82±14 ka	82 ka	82,000	8.2	0.215	Includes 4.0 km^2 of buried lava flow.
Andesite of Crater Butte	Twin Lakes	93±13 ka	93 ka	93,000	17.3	1.73	Includes 1.0 km^2 of buried lava flow.

after about 50 ka. The area covered by regional mafic lava flows is much larger than the area for the Lassen Volcanic Center, but the volume produced is only about a factor of two greater.

Probabilities

An underlying assumption of USGS volcano hazards assessments for Cascade Range volcanoes in Oregon and Washington has been that the probability distribution of time intervals between volcanic eruptions may be treated as a Poisson process. Time histories for some volcanoes elsewhere match this assumption well (for example, Klein, 1982). The probability of an eruption during any particular period of time is calculated from the relation for the occurrence rate. For a Poisson process, this relation is obtained from the exponential distribution for the probability $P\{ T \leq t\}$ that an eruption will occur in a time T less than or equal to the time period t:

$$P\{ T \leq t\} = F(t) = 1 - e^{-\mu t} \quad (1a)$$

$$\approx \mu t , \quad \text{for } \mu t \text{ small}, \quad (1b)$$

where $F(t)$ is the symbol for the probability distribution function and μ is the mean occurrence rate (events per year) for the exponential distribution. Because occurrence rates are low in the Cascades, the approximate relation shown above is normally used (for example, Scott and others, 1995).

Given a set of n time intervals between eruptions t_i, the average recurrence interval (the reciprocal of the occurrence rate) may be determined by:

$$\frac{1}{\mu} = \frac{1}{n} \sum_{i=1}^{n} t_i \ . \quad (2)$$

The properties of a Poisson process include the characteristic that the conditional probability of an eruption occurring within a time period does not depend on the time already waited but only on the time period selected (for example, 1 year, 30 years, or 100 years) to calculate a conditional probability. For some volcanoes, the time history contains disparate time intervals between eruptions, some being short and others much longer. Some examples of time histories having such disparate eruption-time intervals are those of Mount Rainier and Mount St. Helens in Washington. Mullineaux's (1974) data for eruption times of tephra layers at Mount Rainier have three long intervals (>2,000 years) and seven short intervals (<600 years) between eruptions. Mullineaux's (1996) data for Mount St. Helens include one interval of 8,600 years, one of 1,500 years, and 34 of less than 640 years. In such instances, other probability distributions more accurately represent the data, and the conditional probabilities based on those distributions do depend on the time since the last eruption.

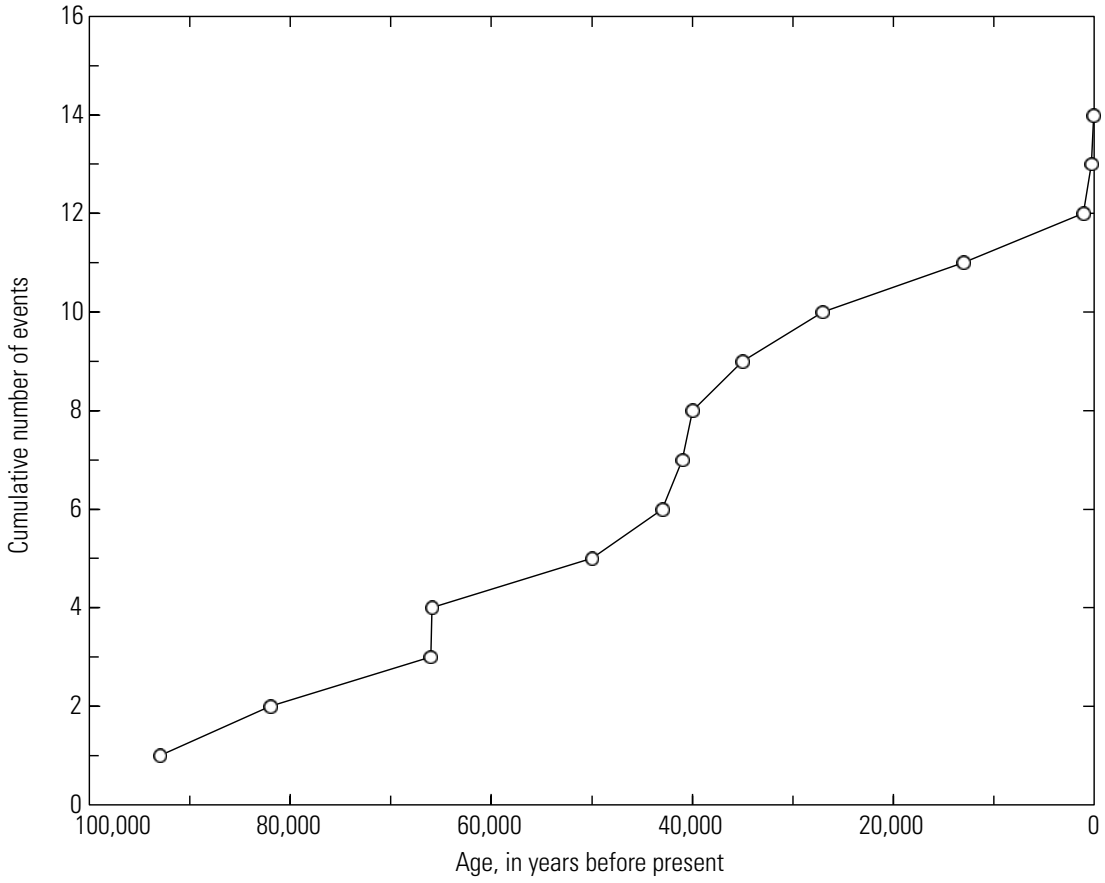

Figure 1. Time history of eruptive events for the Lassen Volcanic Center.

Bebbington and Lai (1996) proposed using the Weibull distribution to match eruption times that vary with the preceding time interval:

$$P\{\ T \le t\} = F(t) = 1 - e^{-\mu(t)}\ , \qquad (3a)$$

Where

$$\mu(t) = \left(\frac{t}{\theta}\right)^{\beta} \qquad (3b)$$

and T is the time, less than the time period t, to the next eruption. Parameters θ and β are referred to as the scale and shape parameters, respectively; when $\beta = 1$, this reduces to the exponential distribution. Several methods are available to estimate θ and β. In a plot of $\ln[\ln(1/(1-F))]$ versus $\ln(t)$, the function is a straight line, and we can estimate the parameters with the best fit to a straight line. A maximum likelihood estimate is obtained by solving the root of a nonlinear equation in β given in Bebbington and Lai (1996). The equation is easily calculated in a spreadsheet, and the value of β is obtained by trial and error.

For eruption intervals that can be divided into two populations, one with short intervals and one with long intervals, a distribution that includes this behavior is the mixed exponential (Cox and Lewis, 1966; Nathenson, 2001):

$$P\{\ T \le t\} = F(t) = 1 - p_1\, e^{-\mu_1 t} - p_2\, e^{-\mu_2 t}\ , \qquad (4)$$

where

$$p_1 = \frac{n_1}{n_1 + n_2} \qquad (5a)$$

and

$$\frac{1}{\mu_1} = \frac{1}{n_1} \sum_{i=1}^{n_1} t_i\ , \qquad (5b)$$

where p_1 is the fraction of short intervals, μ_1 is the average occurrence rate for the short intervals, n_1 is the number of short intervals, and p_2, μ_2, and n_2 are equivalent parameters for the long intervals. The basic notion embodied in the mixed exponential distribution is that there are two states, one involving short intervals and a second involving long intervals. The probability of an eruption occurring in each of these states is governed by an exponential distribution. If one knows that the volcano is currently in a particular state (a difficult judgment to make), then the probability of an eruption can be calculated using the appropriate exponential relation for that state only.

The probability that we are interested in is the conditional probability $P\{\Delta t \le T \le t + \Delta t \mid T > \Delta t\}$ of an eruption occurring between time Δt and time $t + \Delta t$, (for example, during the next year or the next 30 years), after already

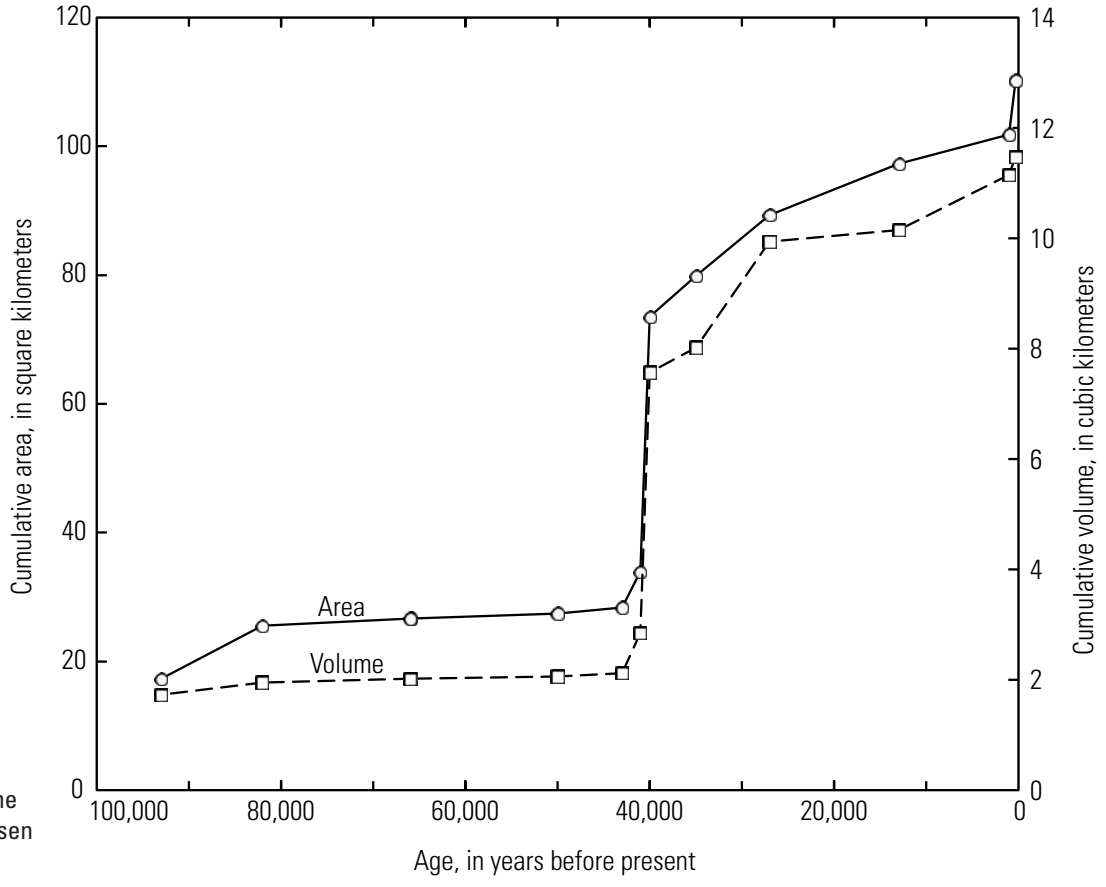

Figure 2. Time history of cumulative area and volume of erupted lava for the Lassen Volcanic Center.

Table 2. Chronology of eruptions less than 100,000 years old for the mafic vents in the surrounding area of the Lassen segment of the Cascade Range.

[Data from Clynne and others (2012). Unit names in italics are from the geologic map of Lassen Volcanic National Park and vicinity (Clynne and Muffler, 2010) and unpublished mapping of the Burney and Lake Almanor quadrangles. Names in roman font are from reconnaissance mapping in the surrounding area. Ages with uncertainties are measured using $^{40}Ar/^{39}Ar$ or K-Ar. Others are estimates constrained by stratigraphy and geomorphology. Age models discussed in text. Areas are calculated from mapped areas of lava flows, and volumes include additions for any associated domes. For parts of lava flows buried by surficial deposits, areas and thicknesses have been estimated, and they are added to the area and volume figures.]

Eruption	Sequence or cluster	Age (ka)	Age - Model I (ka)	Age - Model II (ka)	Area (km^2)	Volume (km^3)	Includes buried lava flow (km^2)
Tholeiitic basalts of Big Lake	Red Lake cluster	50–75	60	74	5.4	0.148	
Basaltic andesite and andesite of Red Lake Mountain[1]	Red Lake cluster	~75	75	75	29.2	0.86	
Basaltic andesite of Red Mountain	Red Lake cluster	75–100	85	76	12.0	0.259	
Andesite of Devils Rock Garden	Tumble Buttes chain	10–15	12	12	7.5	0.57	
Andesite of Bear Wallow Butte	Tumble Buttes chain	35.1±3.1	35.1	35.1	12.5	0.453	
Hall Butte	Tumble Buttes chain	35–50	36	36	5.4	0.144	
Hill 6795	Tumble Buttes chain	35–50	37.5	37.5	1.17	0.0224	
Basaltic andesite of hill 6770	Tumble Buttes chain	35–50	38.5	38.5	2.96	0.085	
Basaltic andesite of Tumble Buttes	Tumble Buttes chain	35–50	39.5	39	2.21	0.074	
Basaltic andesite of hill 5410	Tumble Buttes chain	35–50	40	40.5	1.14	0.0135	0.20
Basaltic andesite of Bear Wallow Butte	Tumble Buttes chain	35–50	42.5	41.5	1.27	0.0211	0.32
Eiler Butte	Tumble Buttes chain	35–50	44	42.5	7.0	0.150	
Basaltic andesite of hill 6138	Tumble Buttes chain	~50	48	49.5	1.30	0.0258	
Basaltic andesite of Section 5	Tumble Buttes chain	~50	50	50	1.94	0.051	
Andesite of Tumble Buttes	Tumble Buttes chain	50–75	71	75.5	5.9	0.059	
Basaltic andesite of Mud Lake	Tumble Buttes chain	75–100	81	76.5	2.27	0.0227	
Andesite of Sugarloaf Peak	Sugarloaf chain	46±7	46.5	46.5	32.4	2.64	
Basaltic andesite of Little Potato Butte	Sugarloaf chain	67±4	67	67	1.05	0.077	
Andesite of Potato Butte	Sugarloaf chain	77±11	77	77	5.7	0.280	
Basaltic andesite of hill 4709	Sugarloaf chain	~80	80	80	0.94	0.0163	
Andesites of Old Station	Sugarloaf chain	75–100	83	81	0.418	0.0167	
Hill 4041	Sugarloaf chain	80–100	86	82.5	0.305	0.0061	
Hill 4899	Sugarloaf chain	80–100	89	83	0.55	0.0201	
Highway 89	Sugarloaf chain	80–100	92	84	0.100	0.00100	
Popcorn Cave	Cinder Butte cluster	30–50	34	37	52	1.75	
Cinder Butte	Cinder Butte cluster	38±7	38	38	38.8	2.59	
Six Mile Hill	Cinder Butte cluster	40–50	43	40	30.8	0.50	
Andesite of Bidwell Spring	Bidwell Spring chain	25–45	28	43	3.75	0.114	1.2
Basaltic andesite of Pole Spring Road	Bidwell Spring chain	25–45	33	44	2.69	0.072	0.30
Basaltic andesite of section 36	Bidwell Spring chain	25–45	41	45	1.20	0.0332	
Basalt of Twin Buttes	Bidwell Spring chain	46±3	46	46	19.8	0.80	
Basaltic andesites of Black Butte	Bidwell Spring chain	~50	49	49	10.7	0.334	2.30
Basaltic andesite of Red Cinder Cone	Red Cinder chain	20–25	21	24.5	1.64	0.054	
Basalt of Red Cinder Cone	Red Cinder chain	20–25	23	25	1.65	0.120	0.57
Basaltic andesite of Red Cinder	Red Cinder chain	25–40	27	26	8.3	0.201	3.5
Basalt of hill 8030	Red Cinder chain	25–40	32	27	7.3	0.178	2.0
Basalt of Cameron Meadow	Red Cinder chain	25–40	37	28	3.92	0.078	3.0
Basalt of Ash Butte	Red Cinder chain	40–70	45	66.5	1.10	0.062	
Basalt of hill 2283	Red Cinder chain	40–70	52	67.5	0.88	0.0292	0.16
Basalt of section 25	Red Cinder chain	40–70	59	68	1.08	0.0185	
Andesite of Red Cinder	Red Cinder chain	69±20	69	69	18.1	1.81	Includes 6.9 km^2 buried lava flow and shield under Red Cinder edifice

Table 2. Chronology of eruptions less than 100,000 years old for the mafic vents in the surrounding area of the Lassen segment of the Cascade Range.—Continued

Eruption	Sequence or cluster	Age (ka)	Age - Model I (ka)	Age - Model II (ka)	Area (km^2)	Volume (km^3)	Includes buried lava flow (km^2)
Basalt east of Ash Butte	Red Cinder chain	70–100	76	69.5	1.19	0.0178	1.0
Basalt of Widow Lake	Red Cinder chain	~100	97	97	0.80	0.0295	0.6
Basaltic andesites of Long Lake	Red Cinder chain	~100	98	98	9.3	0.249	3.6
Basaltic andesite of Caribou Wilderness	Red Cinder chain	~100	99	99	1.20	0.0240	1.0
Basalts of Triangle Lake	Red Cinder chain	~100	100	100	2.70	0.050	0.75
	Miscellaneous group						
Silver Lake[2]	north of Miller Mtn.	10–15	13	13	8.3	0.249	Does not include area of scoria
Twin Buttes	SE of Burney Mtn.	15–25	17	17	10.1	0.296	
Basaltic andesite of Turnaround Lake	Tuya chain	17–35	22	22	0.88	0.079	
Hat Creek Basalt (tholeiitic)	near Old Station	24±6	24	24	99	2.47	
Basaltic andesite of section 32	SE of Twin Buttes	35-50	35	35	1.04	0.0228	
Basalt of junction 4126	NE of Twin Buttes	35-50	42	42	0.300	0.0110	
Basalt of Inskip Hill[3]	Inskip Hill	~50	51	51	62	2.51	
Tholeiitic basalts of Buzzard Springs	near Sifford Mtn.	65±45	65	65	11.1	0.137	0.30
Tholeiitic basalt of Ice Cave Mountain	near Sifford Mtn.	~65	66	66	13.5	0.162	2.6
Basalt of Black Butte	west of Shingletown	~70	70	70	6.5	0.137	Includes 3.8 km^2 of ash
Basalts of Cold Creek Butte	west of Mineral	75–100	82	82	7.1	0.275	1.2
Whittington Place	west of Magee Peak	75–100	90	90	7.9	0.079	

[1] Includes basaltic andesite of Eskimo Hill.

[2] Includes flow at Buckhorn Lake.

[3] Includes Little Inskip Hill, vents at Paynes Creek, and vents in Oak Creek.

waiting a time Δt since the last eruption. It can be shown that this conditional probability can be calculated from the distribution function $F(t)$ as

$$P\{\Delta t \le T \le t + \Delta t \mid T > \Delta t\} = 1 - \frac{1 - F(t + \Delta t)}{1 - F(\Delta t)} \quad . \tag{6}$$

For the simple exponential distribution, the conditional probability reduces to:

$$P\{\Delta t \le T \le t + \Delta t \mid T > \Delta t\} = 1 - e^{-\mu t} \, . \tag{7}$$

Thus, for the simple exponential distribution, the passage of past time does not change the probability of the time to a future eruption. (In the engineering language of time to failure, there is no wear or fatigue). For the Weibull distribution, the conditional probability is:

$$P\{\Delta t \le T \le t + \Delta t \mid T > \Delta t\} = 1 - \exp\left\{\left(\frac{\Delta t}{\theta}\right)^{\beta} - \left(\frac{t + \Delta t}{\theta}\right)^{\beta}\right\} \, . \tag{8}$$

For the mixed exponential, the conditional probability is:

$$P\{\Delta t \le T \le t + \Delta t \mid T > \Delta t\} = 1 - \left[p_1 e^{-\mu_1 (t + \Delta t)} + p_2 e^{-\mu_2 (t + \Delta t)}\right] / \left[p_1 e^{-\mu_1 \Delta t} + p_2 e^{-\mu_2 \Delta t}\right] \, . \tag{9}$$

Thus, in contrast to the simple exponential distribution, the conditional probability for the Weibull and mixed exponential does depend on the time since the last eruption, Δt.

Lassen Volcanic Center

We calculate the time intervals between eruptions for the Lassen Volcanic Center from the eruption chronology in table 1. The time intervals between eruptions are ordered and used to calculate the probability distribution for the data, as shown in figure 7. The time intervals between eruptions systematically increase from hundreds of years to thousands, with the two longest intervals at about 16,000 years. All of the distributions have similar and not very good fits to the data. There is not a significant disparity between long and short intervals between eruptions, and the mixed-exponential distribution is probably not a very good model. The mixed-exponential distribution was fit using eight and five data points so as to have some points as long intervals. The mean and standard deviation of the data are relatively close at 7,150 and 6,110 years, respectively, and one of the properties of the exponential distribution is that the mean and standard deviation are equal. The parameters for the Weibull

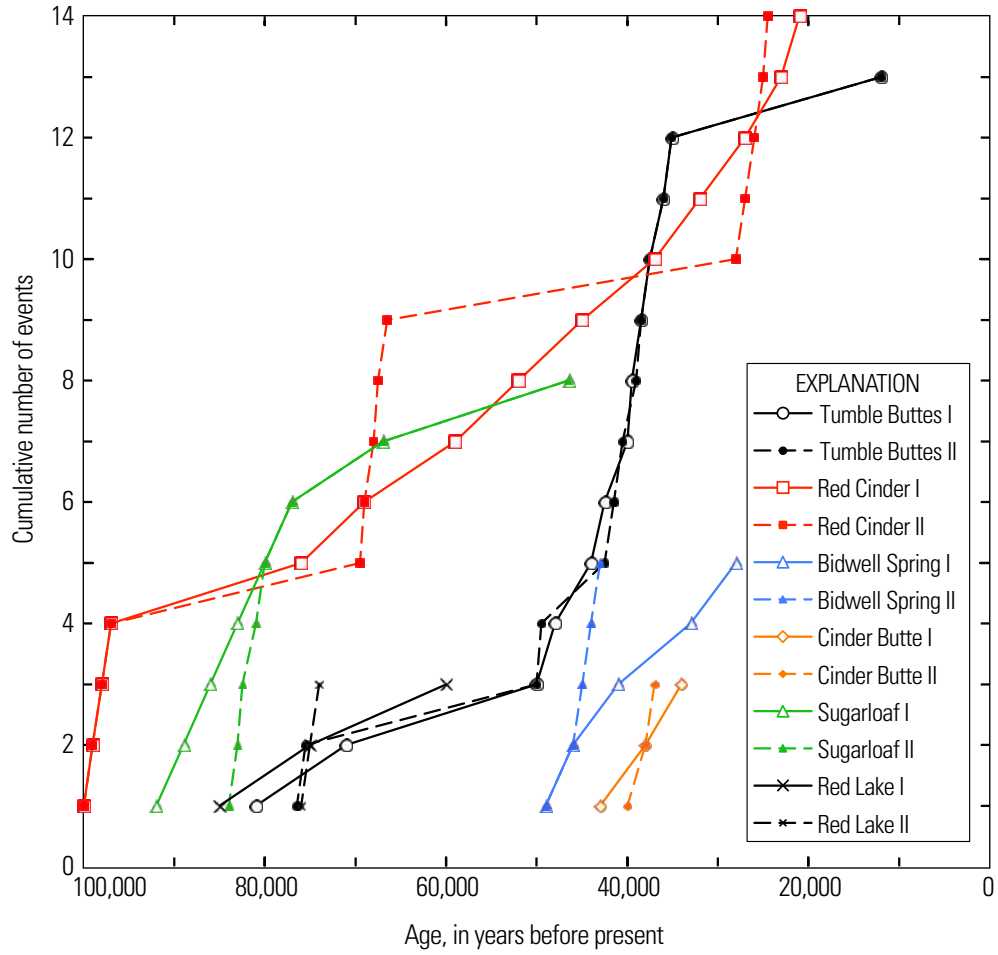

Figure 3. Time history of events for eruptive sequences of regional mafic vents for models I and II. When age and event number coincide for two models in a sequence, the combined symbol becomes a larger filled symbol.

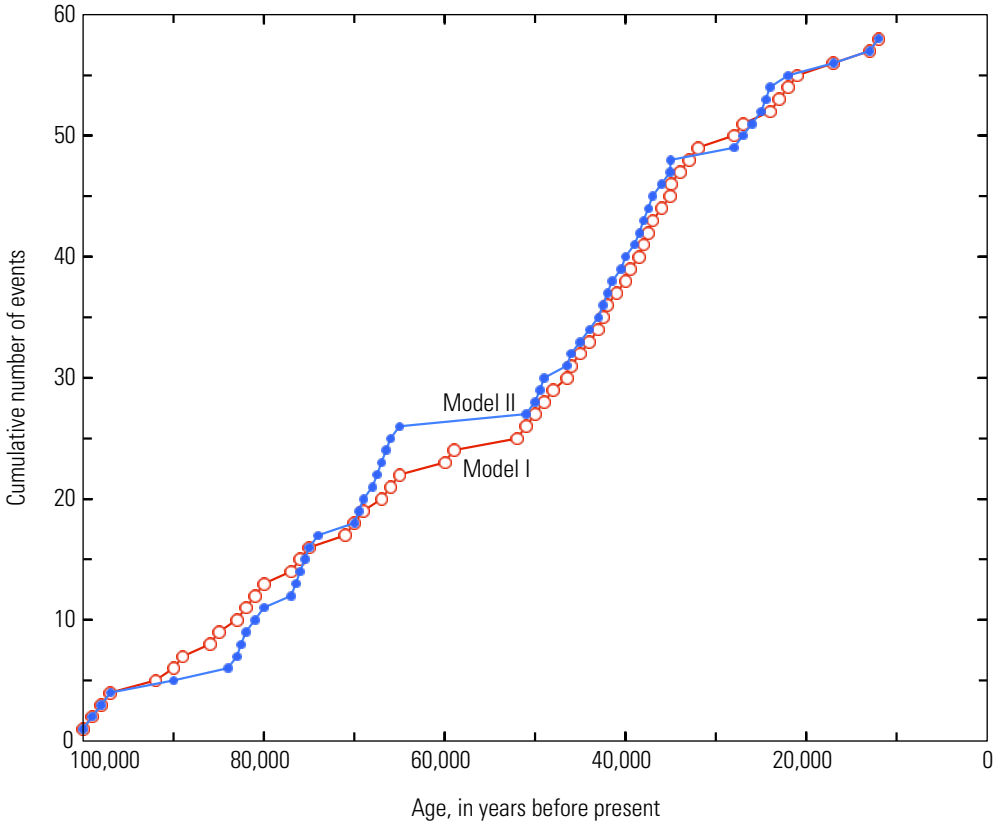

Figure 4. Time history of all eruptive events for regional mafic vents for models I and II.

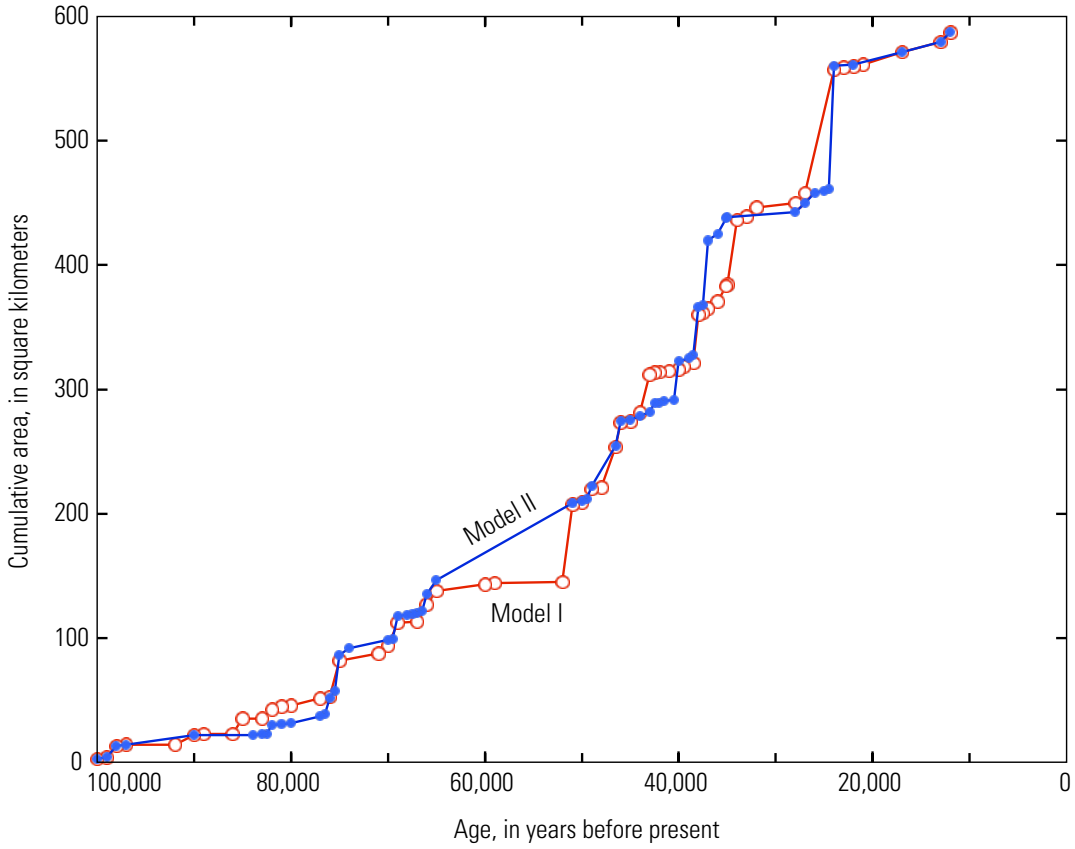

Figure 5. Time history of cumulative area of erupted material for regional mafic vents for models I and II.

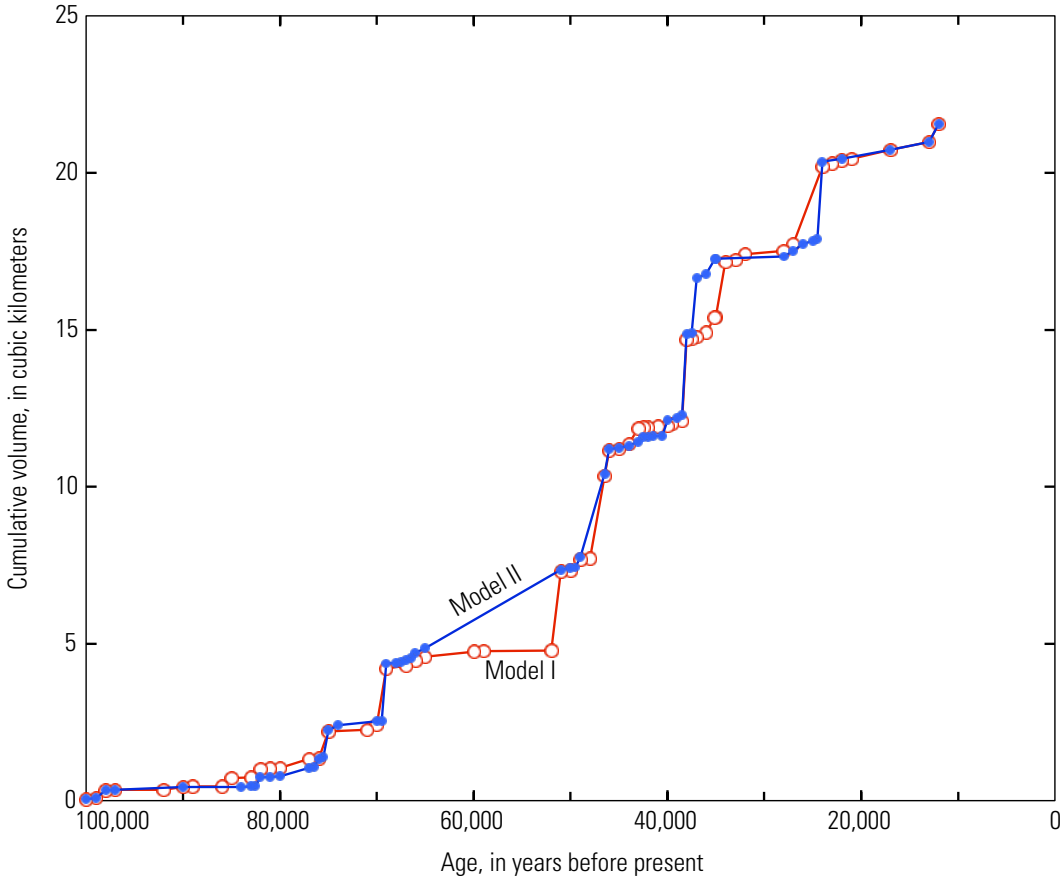

Figure 6. Time history of cumulative volume of erupted material for regional mafic vents for models I and II.

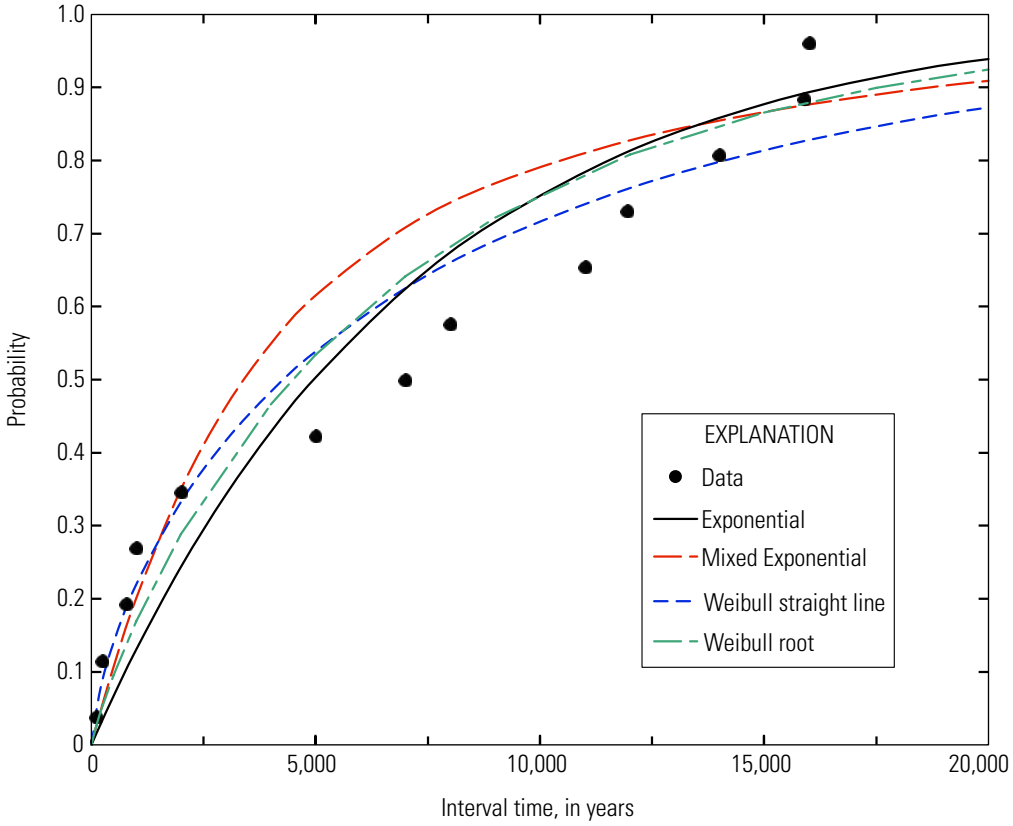

Figure 7. Probability that an eruption will occur in a time less than a given time interval between eruptions. Data from table 1 used to calculate time intervals between eruptions for the Lassen Volcanic Center shown as filled circles, along with curves representing three distributions to match the data. Probabilities for the Weibull distribution shown for parameters for both straight-line and root solutions.

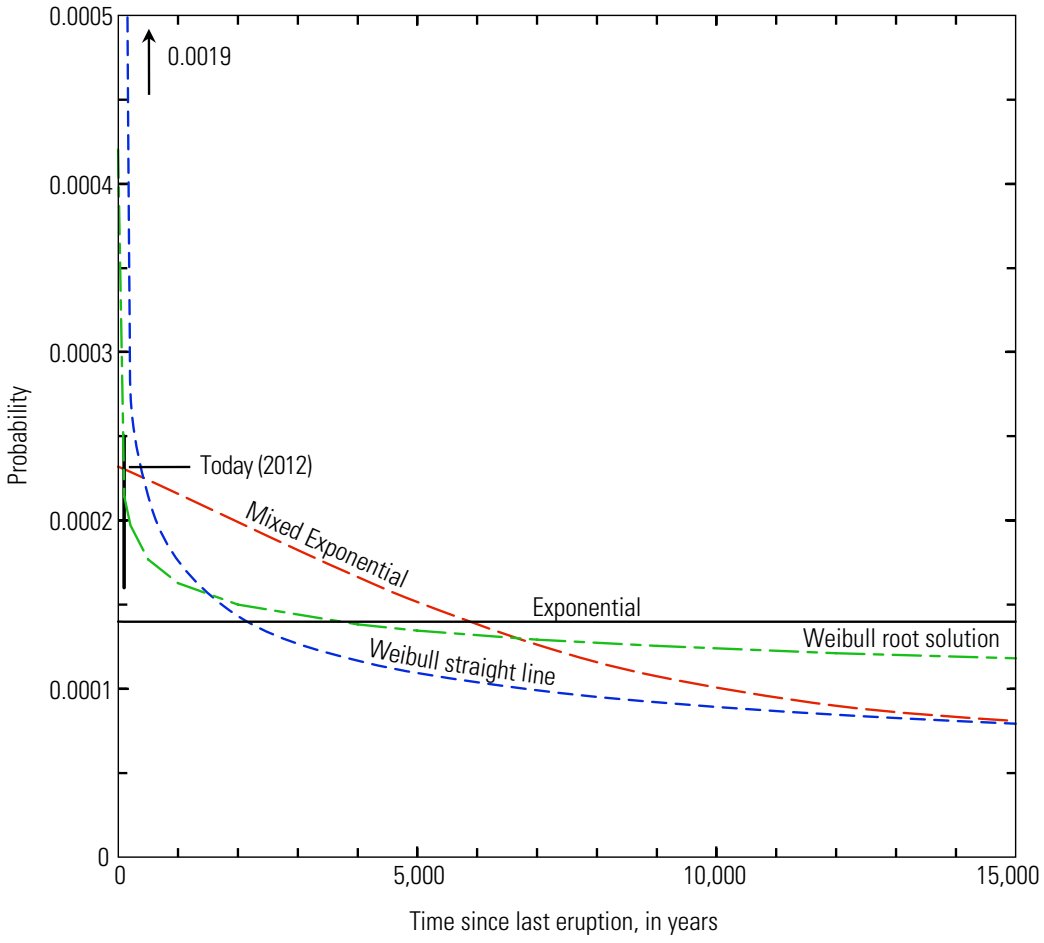

Figure 8. Conditional probability that an eruption will occur at the Lassen Volcanic Center in the next year, given a time since the last eruption. The line marked "today" represents 98 years since the last eruption started in 1914. Conditional probabilities for the Weibull distribution shown for both straight-line and root solutions. At zero time since the last eruption, the Weibull straight-line solution has a value of 0.0019.

distribution have been obtained both by fitting a straight line to the data and through solving the root of an equation by adjusting the value of β until the equation is satisfied (Bebbington and Lai, 1996). The straight-line solution has a β value of 0.707, whereas the root solution has a β value of 0.881. As β gets close to 1, the Weibull behaves more like an exponential distribution (fig. 7). Whether the poor fits of the distributions is a result of the limited size of the dataset (only 13 intervals) or results from some characteristic of the behavior of the Lassen Volcanic Center is unclear.

The conditional probability of an eruption occurring in the next year is given in figure 8 for each of the three distributions. The line marked "today" represents 98 years since the start of the 1914–17 eruption of Lassen Peak. The probability of an eruption occurring in the next year from today is 1.4×10^{-4} for the exponential and 2.3×10^{-4} for the mixed-exponential distribution. The conditional probability for the Weibull distribution using the straight-line fit starts at a value 19×10^{-4} at zero years and has a value of 3.5×10^{-4} at 98 years. For the root solution, the Weibull probability starts at 4.2×10^{-4} and becomes 2.2×10^{-4} at 98 years.

Which distribution should be used to estimate the probability of an eruption today is unclear. The mixed exponential is a better fit to the data for short time intervals (fig. 7) than the exponential distribution. The Weibull distribution using the parameters from the straight-line fit also agrees well with the data for short time intervals (fig. 7), but its rather steep variation in conditional probability in the first few tens of years since the last eruption (fig. 8) is much more extreme than for the root-solution parameters. Because there is some degree of disparity in eruption time intervals (fig. 7), we prefer the mixed-exponential estimate of a probability of 2.3×10^{-4} for an eruption in the next year, recognizing that the exponential value of 1.4×10^{-4} is probably just as valid.

To estimate probabilities for the sizes of future eruptions, the data in table 1 are used to calculate cumulative probabilities of area coverage and volume for lava flows of the Lassen Volcanic Center (fig. 9). The andesite of Eagle

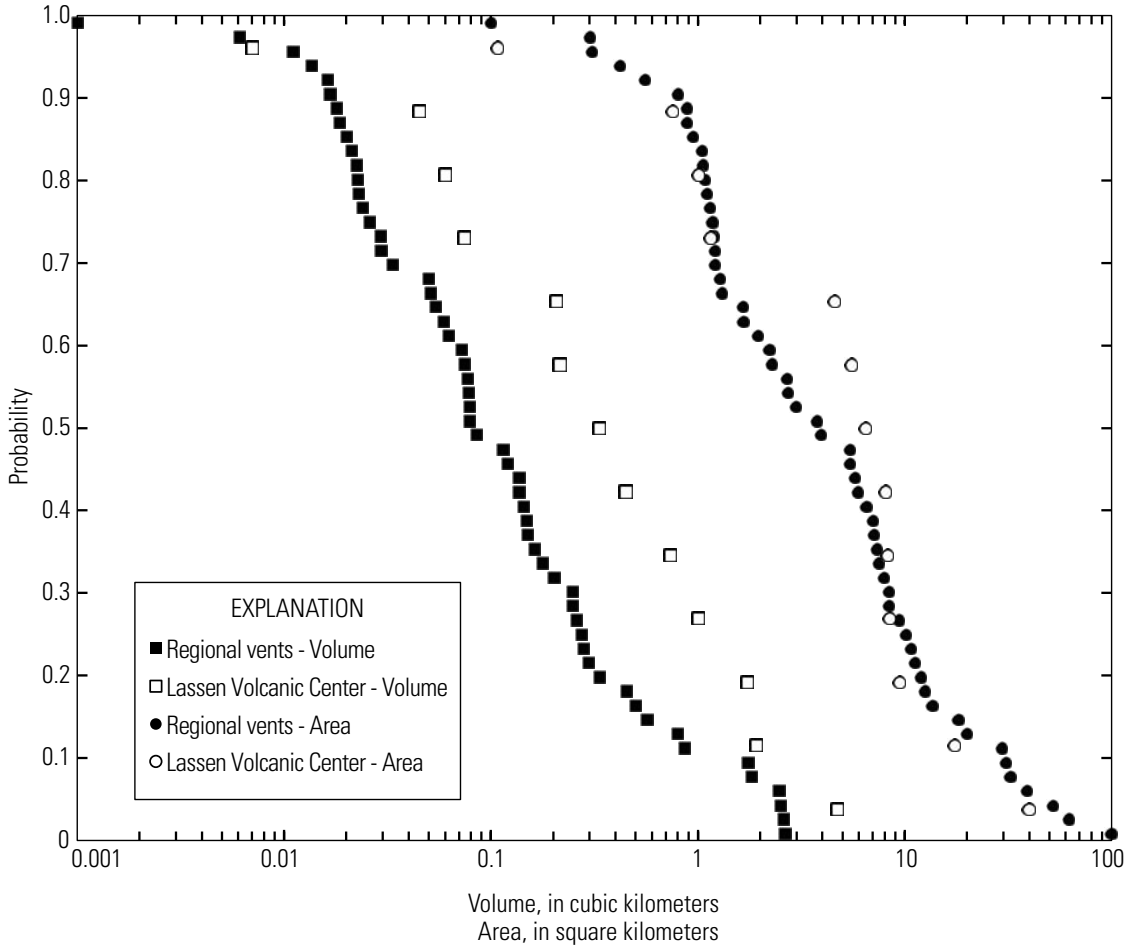

Figure 9. Probability that an eruption in the Lassen Volcanic Center or from a regional mafic vent will have a volume or area greater than a given value.

Peak has been excluded, because it has no associated lava flow. The andesite of Hat Mountain is the largest event in the data; it covered an area of 39.6 km^2 with a volume of 4.72 km^3. The probability of any future eruption producing a lava volume greater than 2 km^3 is about 0.1, whereas the probability that the volume is greater than 0.5 km^3 is about 0.4. The probability that the area covered by lava flow during an eruption will be larger than 17 km^2 is about 0.1, and the probability that the area is larger than 8 km^2 is about 0.4. Thus the potential volumes and areas covered by lava flows in future eruptions are significant. In addition to lava flows, half the eruptions produced pyroclastic flows, and some have included debris flows and pumice fall (table 1). Areas of pyroclastic flows range from 0.02 to 9.4 km^2 (some larger than the associated lava flow), and volumes range from 0.001 to 0.15 km^3. Although the volumes are smaller than most lava flows, the areas covered are significant and the destructive potential greater. Modeling of lahar hazards is described in Robinson and Clynne (2012).

Regional Mafic Vents

Time intervals between eruptions from the regional mafic vents in the surrounding area of the Lassen segment of the Cascade Range are calculated for the two models from the eruption chronology in table 2. The time intervals between eruptions are ordered and used to calculate the probability distribution for the data, as shown in figure 10. Model I has

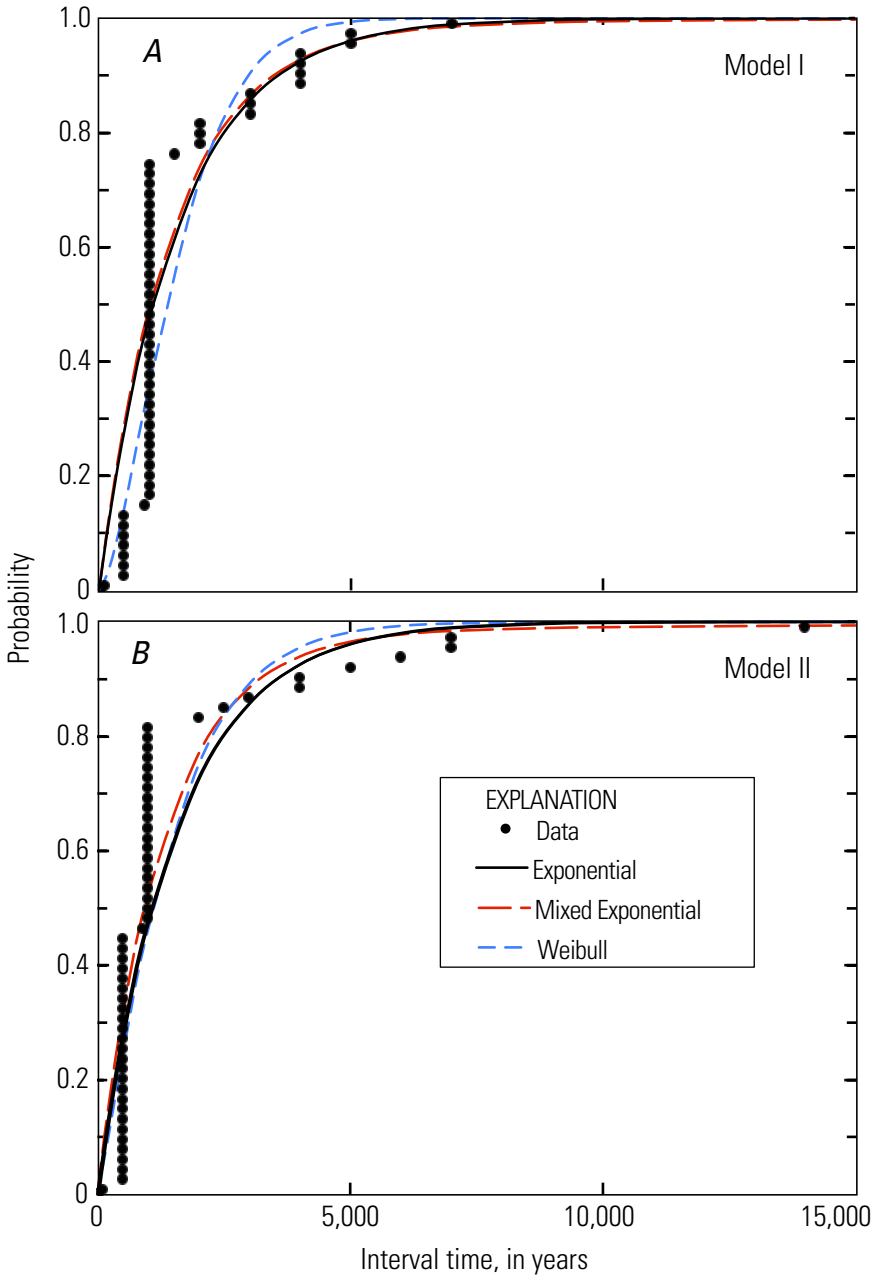

Figure 10. Probability that an eruption will occur at a regional mafic vent in a time less than a given time interval after the previous eruption for model I (*A*) and model II (*B*). Data from table 2 used to calculate time intervals between eruptions for the regional mafic vents, shown as filled circles, along with curves representing three distributions to match the data. Weibull distribution parameters from straight-line solution.

three time intervals between eruptions in the range of 5,000 to 7,000 years, whereas model II has four intervals in the same range and one long interval at 14,000 years (fig. 10). For model I, the exponential distribution is a reasonable fit to the data. The mean and standard deviation of the data are reasonably close at 1,540 and 1,370 years, respectively, consistent with an exponential distribution. The fit to the long-interval data is easier to see in the plot of figure 11 showing $1–F$ on a logarithmic axis, where $F(t)$ is the probability distribution function defined for each of the distributions (equations 1, 3, and 4). In the coordinates of figure 11, the exponential distribution is a straight line. One caution is that the logarithmic scale emphasizes small differences at low values of $1–F$. For model II, all of the probability distributions are reasonably similar fits to the data (fig. 10*B*), and none is a particularly good fit. The mixed exponential is a better fit to the long-time-interval behavior than any of the other distributions (fig. 11*B*).

The estimates of the parameters θ and β for the Weibull distribution (equation 3) are from fitting the best straight line and from the root solution (Bebbington and Lai, 1996). Plotting $\ln\{\ln[1/(1–F)]\}$ against $\ln(t)$ results in a straight line (fig. 12). The values of the parameters can be different from the two methods, but the probability distribution still plots as a straight line in the coordinate system of figure 12. The exponential distribution is the same as a Weibull distribution with the value for β of 1, and it is also a straight line in this coordinate system. Parameter values are given in table 3. For

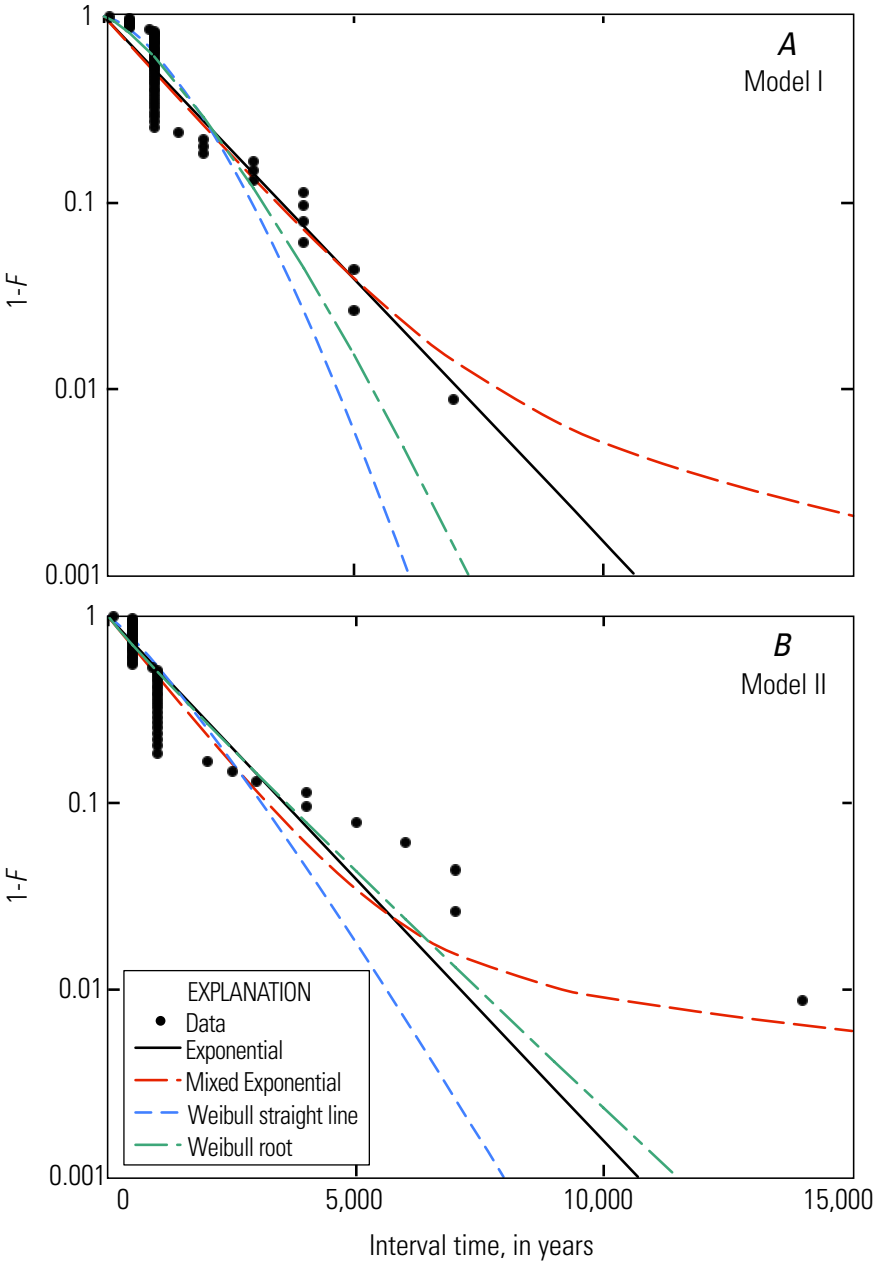

Figure 11. One minus the probability that an eruption will occur at a regional mafic vent in a time less than a given time interval between eruptions (1 - *F*) for model I (*A*) and model II (*B*). Data from table 2 used to calculate time intervals between eruptions, shown as filled circles, along with curves representing three distributions to match the data. Weibull distributions shown for parameters from straight-line and root solutions. Note logarithmic scale. Exponential distribution is a straight line in this coordinate system.

each model, the values of θ from each method of calculation are very similar. The values of the shape parameter β, however, are not. Values of β for model II (which is also the slope in figure 12*B*) that are above and below 1 result in a substantial difference in the conditional probability of an eruption after some time since the last eruption (see below).

The conditional probability of an eruption from the regional mafic vents in the next year after waiting a given time since the last eruption is given in figure 13 for the two models. The probability for the exponential distribution is the same under both models (6.5×10^{-4}) and does not depend on the time since the last eruption. For the mixed exponential, the probability is quite close to the exponential value for several thousand years after the last eruption but becomes significantly lower at longer times, such as today at 12,000 years since the last eruption.

The results for the Weibull distribution are quite sensitive to the shape parameter β (fig. 13). For models I and II at 12,000 years, the results differ by a significant factor within each model for the two solutions and their corresponding values of β. For model I, the variation of the probability with time since the last eruption increases for both values of β (fig. 13*A*). For model II, the variation of the probability with time since the last eruption takes the opposite sense—one increasing and the other decreasing—for the two values of β (fig. 13*B*). For eruption time histories that have short and long intervals, the variation of the conditional probability with increasing time since the last eruption should be decreasing.

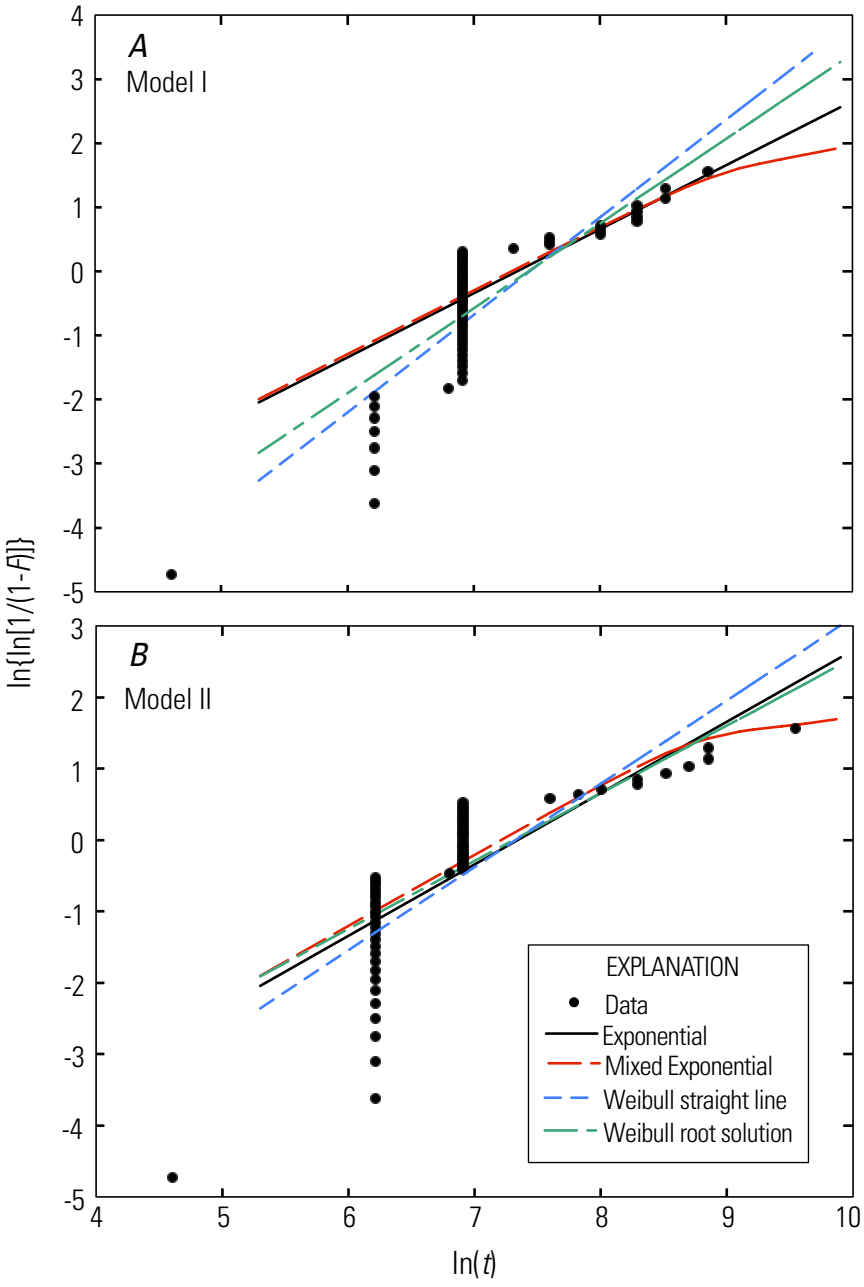

Figure 12. Transformed (Weibull) plot of the probability that an eruption will occur in a time less than a given time interval after the previous eruption for model I (*A*) and model II (*B*). Data shown as filled circles, along with curves representing three distributions to match the data. Weibull distributions shown for parameters from straight-line and root solutions. Exponential and Weibull distributions are straight lines in a Weibull plot.

The varying range in the values of β are because the data in figure 12 are not easily matched by a single straight line.

Because the matches for the mixed-exponential distribution are based on two modeled datasets, the choice for the best estimate of the probability of an eruption today is somewhat problematic. The probability of an eruption today for the exponential distribution is 6.5×10^{-4} and does not depend on the model chosen. Equation 2 can be rewritten to show that the recurrence interval is just the total time span divided by the number of eruptions minus one. Thus, unless some of the eruptions are actually older than 100,000 years, the recurrence interval used in the exponential distribution

Table 3. Parameter values for the Weibull distribution for the straight-line solution and root solution for the eruption chronologies for models I and II for the regional mafic vents.

Model	Method of solution	β	θ (years)
I	Straight line	1.522	1,712
	Root	1.324	1,697
II	Straight line	1.165	1,514
	Root	0.949	1,497

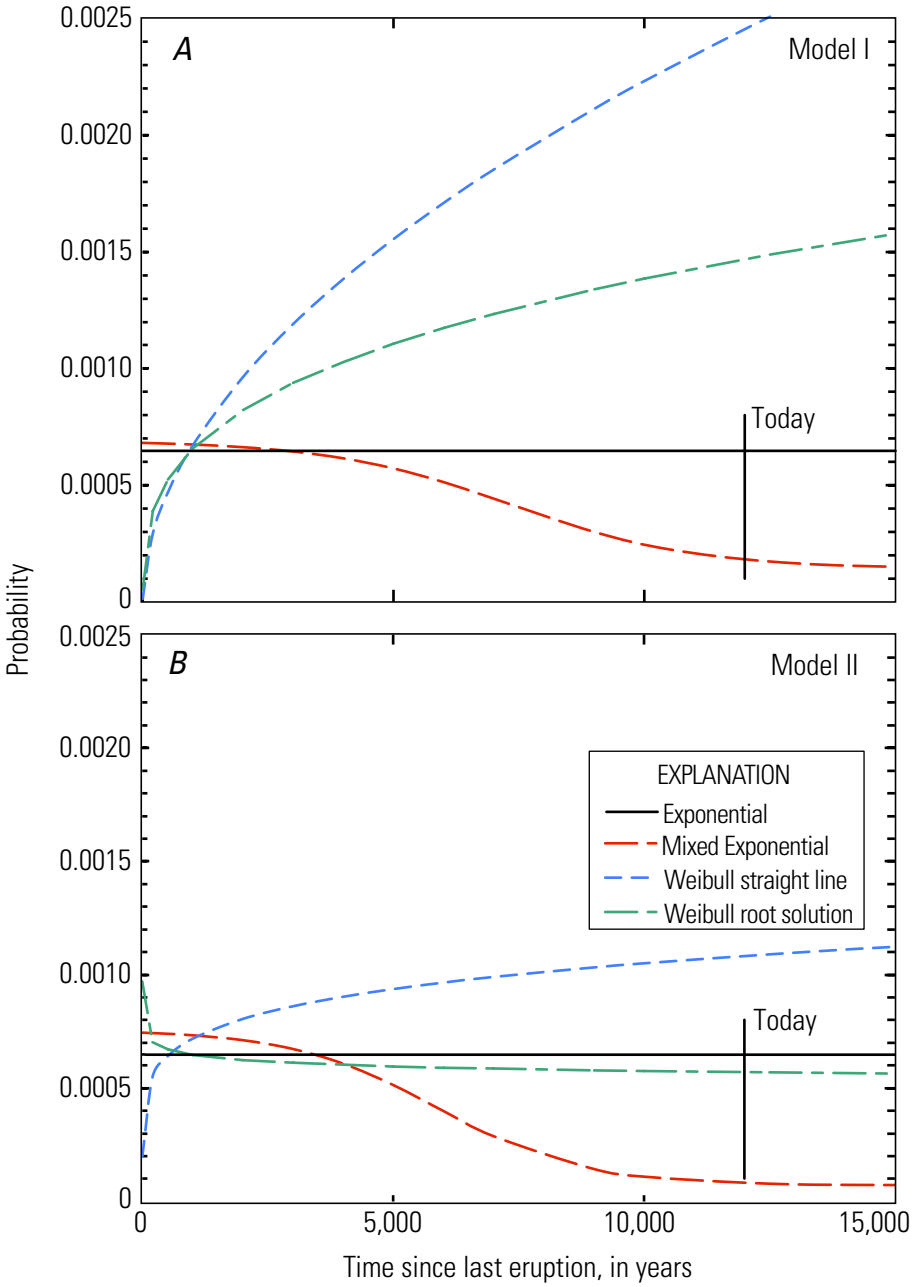

Figure 13. Conditional probability that an eruption will occur from a regional mafic vent in the next year, given a time since the last eruption for model I (*A*) and model II (*B*). The line marked "today" is for 12,000 years, the time since the last eruption. Conditional probabilities for the Weibull distribution shown for parameters for both straight-line and root solutions.

cannot change by much. The results from the mixed-exponential distribution are similar to that for the exponential for times since the last eruption of a few thousand years or less (fig. 13). For long times since the last eruption, such as today where it is 12,000 years, the mixed exponential gives a probability of 1.8×10^{-4} for model I and 0.82×10^{-4} for model II. Given that the data for model I are well matched by the exponential distribution, whereas the data for model II only require the mixed exponential to match the long-time behavior, we chose to use the probability from the exponential distribution of 6.5×10^{-4} for the regional mafic events. However, it should be recognized that the probability 12,000 years after the last event could be much lower. For the exponential distribution, the probability of an eruption from the regional mafic vents (6.5×10^{-4}) is substantially greater than that of an eruption from the Lassen Volcanic Center (1.4×10^{-4}).

To estimate probabilities for the sizes of future eruptions, the data in table 2 are used to calculate cumulative probabilities of area coverage and volume for lava flows from the mafic vents in the surrounding area of the Lassen segment of the Cascade Range (fig. 9). The largest event in the data covered an area of 99 km^2, and the most voluminous event had an erupted volume of 2.64 km^3. The probability of an eruption producing a lava volume greater than 1.3 km^3 is about 0.1, whereas the probability that the volume will be greater than 0.15 km^3 is about 0.4. The probability that the area covered by lava flow during an eruption will be larger than 30 km^2 is about 0.1, and the probability that the area will be larger than 6.7 km^2 is about 0.4. Thus the potential volumes and areas covered by lava flows are significant.

For a given value of probability, the areas covered for the Lassen Volcanic Center are similar to those for the regional mafic vents (fig. 9), whereas the volumes are about a factor of two higher for the Lassen Volcanic Center. This difference may reflect the higher viscosity of the more silicic lavas of the Lassen Volcanic Center compared to the more mafic lavas of the regional vents. One measure of this difference is that the mean area and volume of lava flows for the Lassen Volcanic Center are 8.5 km^2 and 0.88 km^3, whereas the values for the regional vents are 10.1 km^2 and 0.37 km^3. Why the probabilities of areal coverage should be similar is unclear, but the results for Medicine Lake Volcano (Donnelly-Nolan and others, 2007, fig. 17) are similar to those for the mafic vents in the Lassen segment of the Cascade Range, with a mean area of 20.3 km^2 and volume of 0.44 km^3. The mean value for Medicine Lake areas is biased somewhat by the high value for the Giant Crater Flow of 198 km^2, and the distributions are more similar to the Lassen area regional vents than the means indicate.

Probability of Large Explosive Eruptions in the Cascades

The eruptions documented for the past 100,000 years in the Lassen segment of the Cascade arc do not represent the full spectrum of possible eruptions, because no large explosive eruptions have occurred during this period. However, there is clear evidence of several large eruptions within this segment of the arc before 100 ka. The Rockland tephra was erupted at 609±7 ka in the Lassen area, most likely from a source buried by the deposits of Brokeoff Volcano, with a deposit volume of around 120 km^3 and a dense rock equivalent (DRE) volume of around 34 km^3 (table 4). This eruption was much larger than any subsequent eruption in the Lassen area. In addition, a drill hole in the Feather River Meadows, south of Lassen Volcanic National Park, penetrated several hundred feet of ash-flow tuff that correlates with Stage 1 (2.32–1.65 Ma) of the Dittmar volcanic center (Clynne and Muffler, 2010). Ash-flow tuff and other deposits that are correlated with this eruption are found as much as 50 km from the Dittmar volcanic center and are clearly the result of a large eruption. The Nomlaki tuff has a source in the vicinity of the Latour volcanic center (location in Clynne and others, 2012, fig. 3) and was erupted at 3.27 Ma (Poletski, 2010; Harp and Teasdale, 2011). Several other poorly known ash-flow deposits are found in the Lassen area. Thus, the Lassen segment of the Cascade arc has been the site of more than one large explosive eruption over the past several million years.

The Cascades arc presents an array of relatively infrequent large explosive eruptions. A recent event, and one of the largest, was the climactic eruption of Mount Mazama that resulted in the formation of Crater Lake caldera 7,670 cal. yr BP (table 4). Such large explosive eruptions are generally associated with caldera formation. Although it is clear that some volcanic centers are more likely to have large explosive eruptions than others, calculating the probability of such large eruptions for individual volcanoes or volcanic centers does not make much sense. It is not clear which center is the most likely to have a large eruption in the future, and the occurrence at individual volcanic centers is too infrequent to have much confidence in a probability estimate. The sources of some large eruptions in the Cascades are ambiguous (for example, the Shevlin Park Tuff, Oregon) or unknown (Dibekulewe ash), but because the effects of large eruptions are quite widespread, the precise location of the source is less important in terms of hazards. Thus, we focus on calculating the probability of large explosive eruptions for the Cascades arc as a whole.

To estimate this probability, we have chosen a time period of 1.2 m.y. (approximately the age of the eruption that formed Kulshan caldera) as a balance between the likelihood of there being good information (more likely with recent events) and with having a long enough time period to get a reasonable number of occurrences. We have compiled data from the literature (table 4) on eruptions $>\approx5$ km^3 in deposit volume to exclude the relatively frequent eruptions of ~1-2 km^3. A deposit volume of 5 km^3 is ~2 km^3 dense rock equivalent (DRE) for tephra or ~2.5 km^3 DRE for pyroclastic flows. Volume estimates are uncertain, because deposits from some eruptions are not well preserved and others have not been thoroughly studied. Some apparently smaller volume eruptions could potentially be of much larger volume than we

currently know, and thus the frequency could be greater, and some could even be larger than what has been documented for the known large eruptions. For example, layer E from Mount Jefferson is estimated to represent a volume of ~1 km³ DRE by Hildreth (2007), but Beget (1981) suggests that as much as several cubic kilometers of tephra could have been erupted. On the basis of the available data, it is not included in table 4.

In addition to large known eruptions, we include in our compilation the debris avalanche from ancestral Mount Shasta because of its large volume (table 4). The trigger mechanism for this event is unclear, with the possibilities being an unrecognized magmatic intrusion or eruption, an earthquake, a steam explosion from a hydrothermal system, or slope instability from glacial erosion (Crandell, 1989). A recent reconnaissance study of the deposits (David John, written commun., 2011) indicates that hydrothermally altered clasts are sparse and that the debris avalanche contains relatively small amounts of hydrothermal clay minerals, so the source rocks were evidently not weakened by alteration. Whatever the triggering mechanism, the event is related to the presence of a large steep volcanic edifice, justifying its inclusion in the list of large eruptions. It is interesting to note that in a model to explain the presence of slightly thermal springs in the Shasta Valley where the avalanche deposits occur, Nathenson and others (2003) propose the existence of a boiling hydrothermal system in the present edifice of Mount Shasta.

The cumulative numbers of eruptions versus age for the entire dataset in table 4 and for only those events ≥10 km³ are shown in figure 14. For erupted volumes >≈5 km³, 20 events have occurred in the past 1.2 m.y. The plot of all the data shows a high rate of occurrence since 13.6 ka and a much lower rate before then. Most of the events since 13.6 ka are 5–10 km³ in size. Events 10 km³ and larger have occurred at a reasonably constant rate since 630 ka (fig. 14). This gives some confidence that the record of eruptions ≥10 km³ is reasonably complete for that time period. The difference between the two rates of occurrence for volumes >≈5 km³ is probably a result of the poor preservation of deposits for events between 5 and 10 km³ that occurred before the end of the last glaciation at about 15 ka.

Before 630 ka, the only eruptions ≥10 km³ are the Kulshan and Gamma Ridge calderas. This long hiatus, 1150–630 ka, could be real, but it might also be that one or more events in that time period have not been found or studied. Kulshan caldera was identified only in the early 1990s (Hildreth, 1996) and Gamma Ridge caldera only in the past decade (Tabor and others, 2002; Lanphere and Sisson, 2003), and preservation is generally poor for events in the older part of our age range.

For erupted volumes >≈5 km³, we calculate the probability of an eruption from the data for the past 13.6 ka (fig. 15), because data for such eruptions prior to the end of the last glaciation are probably incomplete. There are 7 events and 6 intervals, and the probability is somewhat suspect, because of the large change in rate of occurrence at 13.6 ka (fig. 14). However, the time intervals between eruptions are consistent with an exponential distribution (fig. 16*A*). The average recurrence interval is 2,200 years (equation 2), and the annual probability of a large eruption in the next year is 4.6×10^{-4} (equation 7).

For erupted volumes ≥10 km³, we chose the time period from 630 ka to present. Not including the apparent hiatus from 1.15 Ma to 630 ka makes the calculated probability higher and thus produces a more conservative estimate of the hazard. There are 10 events and 9 intervals, with an average recurrence interval of 70,000 years. The time intervals

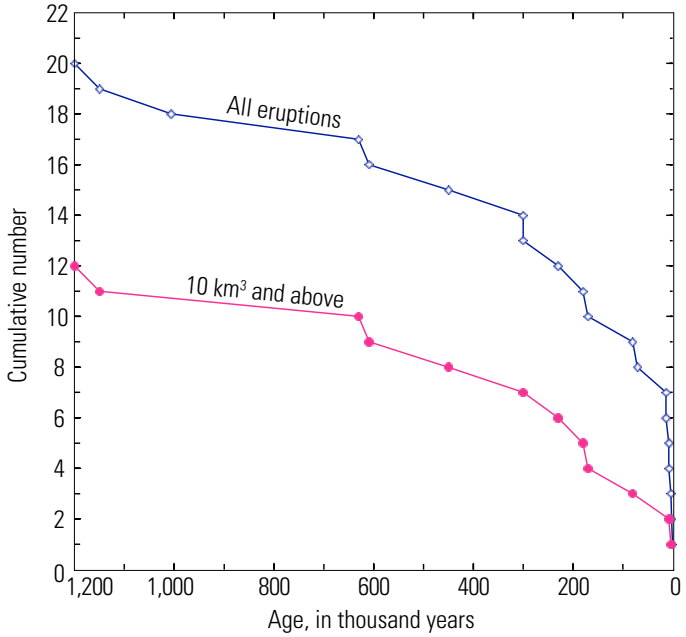

Figure 14. Cumulative number of eruptions versus age for all the data in table 4 with volumes >≈5 km³ and also for only those eruptions with volumes ≥10 km³.

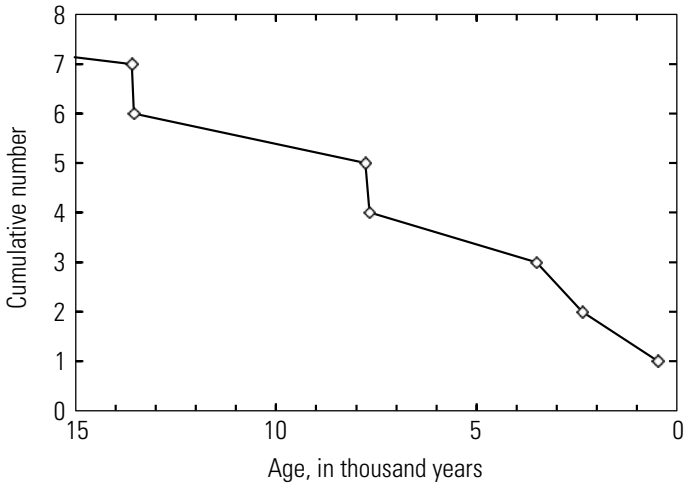

Figure 15. Cumulative number of eruptions versus age for volumes >≈5 km³ for the past 15 thousand years.

Table 4. Compilation of data on large explosive eruptions in the past 1.2 million years in the Cascade volcanic arc.

[Data (arranged north to south) are for Cascade calderas, large tuff deposits, and the Mount Shasta debris avalanche. Where available, both deposit volume and dense rock equivalent (DRE) are given. Data have been compiled for eruptions with deposit volumes ≈5 km^3 and larger. A deposit volume of 5 km^3 is ~2 km^3 DRE for tephra or ~2.5 km^3 DRE for pyroclastic flows, except where different densities are used in original study. Calibrated radiocarbon ages (cal. yr BP) are in years before present (1950 C.E.). Older ages are in thousands of years (ka) or millions of years (Ma). Uncertainties are ±1 σ except where noted. Est., estimated.]

Eruption	Age	Deposit volume (km^3)	DRE volume (km^3)	Notes and references
Bridge River tephra – Mount Meager	2,360 cal. yr BP (2,700–2,350 ±2 σ)		2	Clague and others (1995), Hildreth (2007).
Kulshan caldera – east of Mount Baker	1.15 ± 0.01 Ma		~ 30	Correlates with Lake Tapps tephra. Hildreth (1996), Hildreth and others (2004), Hildreth (2007).
Glacier Peak - layer B	13.55 ka	6.5	2.1	A few decades younger than layer G (Kuehn and others, 2009). Volume 6.5 km^3 using scaled volume method of Carey and others (1995), 2.1 km^3 DRE (Gardner and others, 1998).
Glacier Peak - layer G	13.6 ka (13.7 – 13.5)	6.0	1.9	13,660–13,490 cal. yr BP (Kuehn and others, 2009). Volume 6 km^3 using scaled volume method of Carey and others (1995), 1.9 km^3 DRE (Gardner and others, 1998).
Gamma Ridge caldera – northeast of Glacier Peak	~1.2 Ma		~40	Volcanic rocks of Gamma Ridge recognized as from a caldera forming eruption by Tabor and others (2002), and the name appears in Lanphere and Sisson (2003) and Haugerud and Tabor (2009). K-Ar age for andesite/dacite lava within the volcanic rocks of Gamma Ridge is 1.242±0.024 Ma, and age of unconformable lava on top from Glacier Peak is 616±14 ka (T.W. Sisson and M.A. Lanphere, written commun., 2011). Assume ~1.2 Ma as a reasonable age for caldera formation. Proposed to be a trap-door caldera (Lipman, 1997) with the dropped portion defined by the arc of the Suiattle River (T.W. Sisson, oral commun., 2011), approximately a semicircle with a radius of 7 km. Assuming the older rocks in the Suiattle River drainage dropped to about their present elevation (Tabor and Crowder, 1969), the greatest downdrop is 1,200 m. Volume from spherical wedge.
Layer Wn – Mount St. Helens	1479 C.E.	7.7	2	Kalama period 1479 C.E. (Yamaguchi and Hoblitt, 1995). Volume 7.7 km^3, 2 km^3 DRE using scaled volume method (Carey and others, 1995).
Layer Yn – Mount St. Helens	3.5 ka	15	4	Smith Creek period ~3,500 cal. y BP (Clynne and others, 2005). Volume 15 km^3, 4 km^3 DRE using scaled volume method (Carey and others, 1995).
Basaltic andesite lapilli tuff – Olema ash - formation of Newberry caldera	~80 ka		14-22	Est. age 80 ka (Donnelly-Nolan and others, 2004). >5? km^3 DRE (Hildreth, 2007), but MacLeod and others (1995) propose >10 km^3 DRE (see also MacLeod and Sherrod, 1988). For a 7 x 5 km caldera (MacLeod and others, 1995), an ellipse of that size has an area of 27 km^2. For a caldera block downdrop of 500–800 m (MacLeod and others, 1995), the volume is 14–22 km^3 DRE. Recent work by J. Donnelly-Nolan (oral commun., 2011) indicates that the downdrop is likely to be significantly larger.
Tuff of Tepee Draw – Newberry caldera	230 ka	Several tens	~10 ?	Formation of earlier Newberry caldera (Jensen and others, 2009). Est. age 230 ka (J. Donnelly-Nolan, written commun., 2011; Donnelly-Nolan and others, 2004). ~10? km^3 DRE (Hildreth, 2007), MacLeod and Sherrod (1988) estimate that several tens of cubic kilometers erupted.
Tuff of Brooks Draw – near Newberry	300 ka	2.4–4.8		Est. age 300 ka (J. Donnelly-Nolan, written commun., 2011; Jensen, 2009). Maximum exposed thickness 20 m (MacLeod and others, 1995). Tuff of Brooks Draw (Jensen and others, 2009) combines tuff of Orphan Butte and dacitic tuff of MacLeod and others (1995) into a single unit. Tuff is 10 m thickness 15 km from likely source at center of caldera (J. Donnelly-Nolan, written commun., 2011); outcrop area is about 8 km in width at 10–14 km from the center of the caldera. Assuming 12 km in width, 20 km length, and 10–20 m in thickness, volume is 2.4–4.8 km^3 or 1.2–2.4 km^3 DRE.
Shevlin Park Tuff – source west of Bend	~0.17 Ma		>5	Younger than Tumalo Tuff; thought to be younger than 0.17 Ma (Sherrod and others, 2004). Conrey and others (2001) propose an alternate age of ~260 ka. Volume >5 km^3 DRE (Hildreth, 2007).
Bend Pumice and Tumalo Tuff	0.3±0.1 Ma		>5?	Correlated with Loleta ash. Source west of Bend. Age is 0.4–0.3 Ma; weighted mean of four ages 0.3±0.1 Ma (Sherrod and others, 2004). >5? km^3 DRE (Hildreth, 2007).
Crater Lake – climactic eruption of Mount Mazama	7,670 cal. yr BP (7,790–7,590 ±2 σ)	142	47	7,670 cal. yr BP (Nathenson and others, 2007). Erupted volume of air-fall tephra 117 km^3 and ash-flow deposits 25 km^3; magma volume of explosive products 47 km^3 DRE (Bacon, 1983).
Llao Rock pumice fall – Crater Lake	7,770 cal. yr BP		2.5	Correlates with Tsoyowata ash bed. Age 100–200 years before climactic eruption of Mount Mazama. Volume 2.5 km^3 DRE (Bacon and Lanphere, 2006).
Pumice Castle – Crater Lake	71±5 ka		2	Pyroclastic flow and ash fall 2 km^3 DRE (Bacon and Lanphere, 2006).

Table 4. Compilation of data on large explosive eruptions in the past 1.2 million years in the Cascade volcanic arc.—Continued

Eruption	Age	Deposit volume (km^3)	DRE volume (km^3)	Notes and references
Mount Shasta debris avalanche	450±75 ka	45		Age bracketed by Rockland tephra occurring in the deposit (Crandell, 1989) with an age of 609±7 ka (Lanphere and others, 2004) and the deposit being younger than Sargents Ridge episode of Mount Shasta with an oldest age of 290 ka (A.T. Calvert, oral commun., 2011). Ages of blocks in the deposit are 360±40 ka and 380±60 ka, and age of basalt lava flow overlying deposit is 300±100 ka (Crandell, 1989); accuracy of reported ages is suspect. We propose an estimated age of 450±75 ka (± 1 σ) covering the range of possible ages with ± 150 ka (± 2 σ). Volume of 45 km^3 extending 49 km from source and up to 13 km in width (Crandell, 1989).
Tuff of Antelope Well – formation of Medicine Lake caldera	~180 ka		~20	Age of ~180 ka (Donnelly-Nolan and others, 2008). Volume 10 km^3 DRE (Donnelly-Nolan and others, 2008). For a 7 x 12 km caldera (Donnelly-Nolan and others, 2008), an ellipse of that size has an area of 66 km^2. For a caldera block downdrop of 240–440 m (Donnelly-Nolan and others, 2008), the volume is 16–29 km^3 DRE.
Older tuff of Box Canyon – near Medicine Lake	1.006±0.025 Ma	4.5		Age of 1.006±0.025 Ma (Donnelly-Nolan, 2010). 10 m thickness north of Medicine Lake with a possible source from Medicine Lake or from an area to the southwest between Shasta and Medicine Lake near Red Cap Mountain (Donnelly-Nolan, 2010). Outcrop area is about 11 km in width at around 23 km from the caldera center or area of older rhyolite of Red Cap Mountain. Assuming 15 km in width, 30 km length, and an average thickness of 10 m, volume is 4.5 km^3 or 2.3 km^3 DRE.
Rockland tephra – in Lassen area	609±7 ka	~120		Caldera likely buried by Brokeoff Volcano (Clynne and Muffler, 2010). Age 609±7 ka (Lanphere and others, 2004). Volume > 30 km^3 DRE (Hildreth, 2007). Volume ~50 km^3 DRE based on comparison of thickness versus distance to Mazama ash (Sarna-Wojcicki and others, 1985). Based on Sarna-Wojcicki and others (1985) comparing thickness of Rockland tephra to Mazama ash, Rockland tephra volume should be ~120 km^3 deposit volume and 35 km^3 DRE.
Dibekulewe ash – south central Cascades	~630 ka		>5?	Source area not known; widespread in California, Nevada, and Oregon. Age ~630 ka and volume >5? km^3 DRE (Hildreth, 2007).

between eruptions are consistent with an exponential distribution (fig. 16*B*). The occurrence of sequences of two eruptions relatively close in time separated by longer periods of no activity (fig. 14) may be something of an artifact of the inadequacies of the dating for some of the eruptions, but these short time intervals are also consistent with an exponential distribution (fig. 16*B*). The annual probability of a large eruption in the next year is 1.4×10^{-5}. Although there have been two events in the Holocene (Layer Yn at Mount St. Helens and the climactic eruption of Mount Mazama to form Crater Lake caldera), the previous event was the formation of Newberry caldera at 80 ka. By focusing on a relatively long time period and the largest eruptions in the Cascades, we have some confidence that the resulting probability is a reasonable estimate.

Conclusion

Data for chronologies of eruptive activity at the Lassen Volcanic Center and for eruptions from the regional mafic vents in the surrounding area of the Lassen segment of the Cascade Range have been compared to three probability distributions to estimate probabilities of future eruptions. The choices of best estimates are not clear cut, because there is no clear best matching probability distribution for data from the Lassen Volcanic Center and because the calculations for the regional mafic vents depend on which model is used in developing the chronology. For the Lassen Volcanic Center, we prefer the estimate from the mixed-exponential distribution of a probability of 2.3×10^{-4} for an eruption in the next year, recognizing that the value of 1.4×10^{-4} derived using the exponential distribution is probably just as valid. For the regional mafic vents, we prefer the probability from the exponential distribution of 6.5×10^{-4}, because it is not model dependent. The probability of an eruption from a regional mafic vent is substantially higher than that of an eruption from the Lassen Volcanic Center, even though there has not been a regional event since 15,000–10,000 years ago. If the chronology for the regional mafic vents were better known, we would not need to propose models to develop a detailed chronology, and the estimate of the probability of an eruption could be better defined.

The analysis of the probability of large explosive eruptions in the Cascade Range was done both for erupted volumes $>\approx5$ km^3 and for volumes ≥10 km^3. In order to gain some perspective on the relative magnitudes of probabilities calculated in this study, figure 17 shows those values along with some values from other studies for probabilities of various events in the Cascades. For Medicine Lake Volcano in the year after an eruption and for Mount St. Helens in its

currently active period for an explosive eruption ≥0.1 km³, the values are around a probability of 10^{-2} per year. The probability of an eruption anywhere in the U.S. portion of the Cascades has a similar but somewhat higher value. For longer term histories, probabilities are mostly in the range 2×10^{-4} to 2×10^{-3}, including those for the Lassen Volcanic Center and the Lassen regional mafic vents. The current probability of an eruption from Medicine Lake volcano, 947 years after the last eruption, is also within this range. The probability of an explosive eruption in the Cascades with a volume >≈5 km³ is within this range as well. For an explosive eruption in the

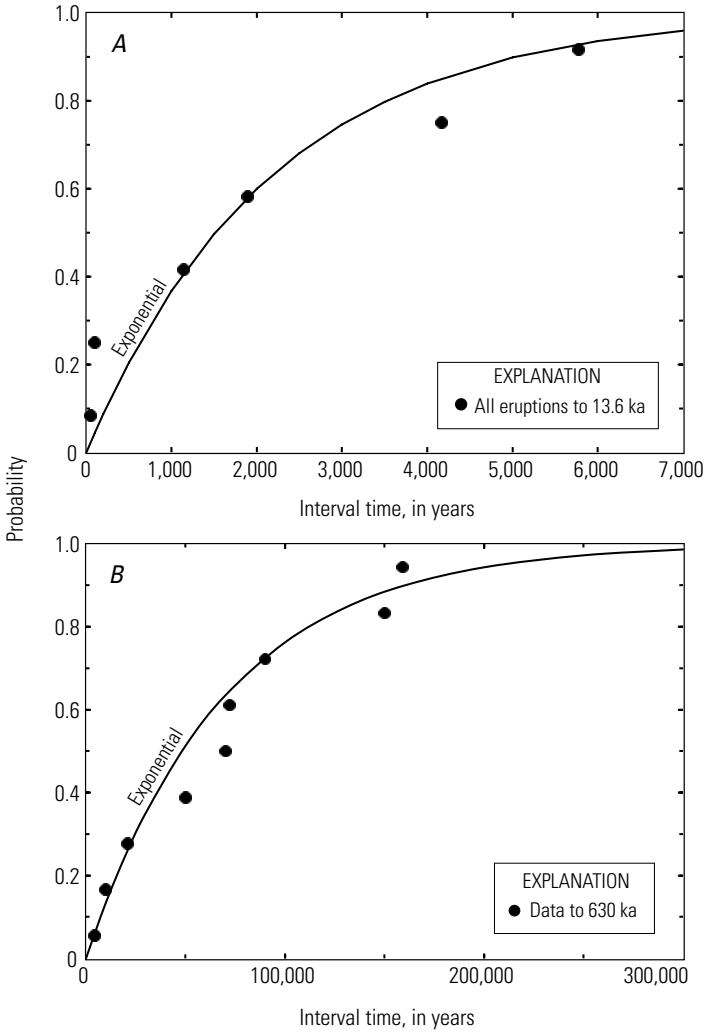

Figure 16. Probability that an eruption will occur in a time less than a given time interval since the previous eruption for volumes >≈5 km³ back to 13.6 ka (*A*) and for volumes ≥10 km³ back to 630 ka (*B*). Data for time intervals between eruptions shown as filled circles, along with the curve for an exponential distribution that matches the data.

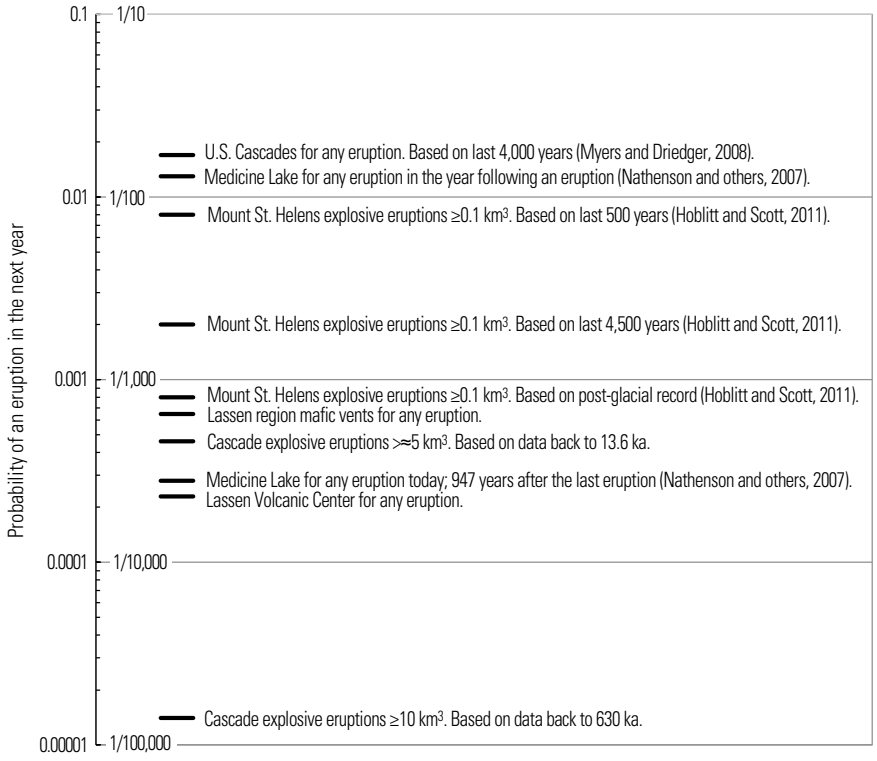

Figure 17. Probability of an eruption in the next year for various events in the Cascades. Values shown as both decimals and fractions on logarithmic scale.

Cascades with a volume ≥10 km^3, the probability is distinctly less than for these other events.

Acknowledgements

Julie Donnelly-Nolan, Thomas Sisson, Charles Bacon, and Andrew Calvert are thanked for useful discussions on large eruptions. William E. Scott and John W. Ewert provided helpful reviews.

References Cited

Bacon, C.R., 1983, Eruptive history of Mount Mazama and Crater Lake caldera, Cascade Range, U.S.A.: Journal of Volcanology and Geothermal Research, v. 18, p. 57–115.

Bacon, C.R., and Lanphere, M.A., 2006, Eruptive history and geochronology of Mount Mazama and the Crater Lake region, Oregon: Geological Society of America Bulletin, v. 118, p. 1331–1359.

Bebbington, M.S., and Lai, C.D., 1996, On nonhomogeneous models for volcanic eruptions: Mathematical Geology, v. 28, p. 585–600.

Beget, J.E., 1981, Evidence of Pleistocene explosive eruptions of Mount Jefferson, Oregon [abs.]: Eos (American Geophysical Union Transactions), v. 62, no. 45, p. 1089.

Carey, S., Gardner, J., and Sigurdsson, H., 1995, The intensity and magnitude of Holocene plinian eruptions from Mount St. Helens volcano: Journal of Volcanology and Geothermal Research, v. 66, p. 185–202.

Christiansen, R.L., Lowenstern, J.B., Smith, R.B., Heasler, H., Morgan, L.A., Nathenson, M., Mastin, L.G., Muffler, L.J.P., and Robinson, J.E., 2007, Preliminary assessment of volcanic and hydrothermal hazards in Yellowstone National Park and vicinity: U.S. Geological Survey Open-File Report 2007–1071, 94 p. [http://pubs.usgs.gov/of/2007/1071/].

Clague, J.J., Evans, S.G., Rampton, V.N., and Woodsworth, G.J., 1995, Improved age estimates for the White River and Bridge River tephras, western Canada: Canadian Journal of Earth Sciences, v. 32, p. 1172–1179.

Clynne, M.A., and Muffler, L.J.P., 2010, Geologic map of Lassen Volcanic National Park and vicinity, California: U.S. Geological Survey Scientific Investigations Map 2899, 116 p., 3 plates, scale 1:50,000, CD-ROM [http://pubs.usgs.gov/sim/2899/].

Clynne, M.A., Ramsey, D.W., and Wolfe, E.W., 2005, Pre-1980 eruptive history of Mount St. Helens, Washington: U.S. Geological Survey Fact Sheet 2005-3045, 4 p.

Clynne, M.A., Robinson, J.E., Nathenson, M., and Muffler, L.J.P., 2012, Volcano hazards assessment for the Lassen region, northern California: U.S. Geological Survey Scientific Investigations Report 2012-5176-A, 47 p., 1 plate [http://pubs.usgs.gov/sir/2012/5176/a/].

Conrey, R.M., Donnelly-Nolan, J., Taylor, E.M., Champion, D., and Bullen, T., 2001, The Shevlin Park tuff, Central Oregon Cascade Range; magmatic processes recorded in an arc-related ash-flow tuff [abs.]: Eos (American Geophysical Union Transactions), Fall meeting supplement, v. 82, no. 47, abs. V32D-0994.

Cox, D.R., and Lewis, P.A.W., 1966, The statistical analysis of series of events: London, Methuen, 285 p.

Crandell, D.W., 1989, Gigantic debris avalanche of Pleistocene age from ancestral Mount Shasta volcano, California, and debris-avalanche hazard zonation: U.S. Geological Survey Bulletin 1861, 32 p.

Donnelly-Nolan, J.M., 2010, Geologic map of Medicine Lake volcano, northern California: U.S. Geological Survey Scientific Investigations Map 2927, 48 p., 2 plates, scale 1:50,000, CD-ROM.

Donnelly-Nolan, J.M., Champion, D.E., Lanphere, M.A., and Ramsey, D.W., 2004, New thoughts about Newberry Volcano, central Oregon, USA [abs.]: Eos (American Geophysical Union Transactions), v. 85, no. 47, Fall meeting supplement, abs. V43E-1452.

Donnelly-Nolan, J.M., Nathenson, M., Champion, D.E., Ramsey, D.W., Lowenstern, J.B., and Ewert, J.W., 2007, Volcano hazards assessment for Medicine Lake volcano, northern California: U.S. Geological Survey Scientific Investigations Report 2007–5174–A, 26 p., 1 plate [http://pubs.usgs.gov/sir/2007/5174/a/].

Donnelly-Nolan, J.M., Grove, T.L., Lanphere, M.A., Champion, D.E., and Ramsey, D.W., 2008, Eruptive history and tectonic setting of Medicine Lake Volcano, a large rear-arc volcano in the southern Cascades: Journal of Volcanology and Geothermal Research, v. 177, p. 313–328.

Gardner, J.E., Carey, S., and Sigurdsson, H., 1998, Plinian eruptions at Glacier Peak and Newberry volcanoes, United States; implications for volcanic hazards in the Cascades: Geological Society of America Bulletin, v. 110, p. 173–187.

Guffanti, M., Clynne, M.A., and Muffler, L.J.P., 1996, Thermal and mass implications of magmatic evolution in the Lassen volcanic region, California, and minimum constraints on basalt influx to the lower crust: Journal of Geophysical Research, v. 101, p. 3003–3013

Harp, A., and Teasdale, R., 2011, Locating the source of the Nomlaki tuff [abs.]: Geological Society of America Abstracts with Programs, v. 43, no. 4, p. 67.

Haugerud, R.A., and Tabor, R.W., 2009, Geologic map of the North Cascade Range, Washington: U.S. Geological Survey Scientific Investigations Map 2940, 23 p., 2 plates, scale 1:200,000, CD-ROM.

Hildreth, W., 1996, Kulshan caldera—a Quaternary subglacial caldera in the North Cascades, Washington: Geological Society of America Bulletin, v. 108, p. 786–793.

Hildreth, Wes, 2007, Quaternary magmatism in the Cascades—geologic perspectives: U.S. Geological Survey Professional Paper 1744, 125 p.

Hildreth, W., Lanphere, M.A., Champion, D.E., and Fierstein, J., 2004, Rhyodacites of Kulshan caldera, North Cascades of Washington; postcaldera lavas that span the Jaramillo: Journal of Volcanology and Geothermal Research, v. 130, p. 227–264.

Hoblitt, R.P., and Scott, W.E., 2011, Estimate of tephra accumulation probabilities for the U.S. Department of Energy's Hanford Site, Washington: U.S. Geological Survey Open-File Report 2011–1064, 15 p.

Jensen, R.A., Donnelly-Nolan, J.M., and Mckay, D., 2009, A field guide to Newberry Volcano, Oregon, *in* O'Connor, J.E., Dorsey, R.J., and Madin, I.P., eds., Volcanoes to vineyards—geologic field trips through the dynamic landscape of the Pacific Northwest: Geological Society of America Field Guide 15, p. 53–79.

Klein, F.W., 1982, Patterns of historical eruptions at Hawaiian volcanoes: Journal of Volcanology and Geothermal Research, v. 12, p. 1–35.

Kuehn, S.C., Froese, D.G., Carrara, P.E., Foit, F.F., Jr., Pearce, N.J.G., and Rotheisler, P., 2009, Major- and trace-element characterization, expanded distribution, and a new chronology for the latest Pleistocene Glacier Peak tephras in western North America: Quaternary Research, v. 71, p. 201–216.

Lanphere, M.A., and Sisson, T.W., 2003, Episodic volcano growth at Mt. Rainier, Washington—a product of tectonic throttling? [abs.]: Geological Society of America Abstracts with Programs, v. 35, no. 6, p. 644.

Lanphere, M.A., Champion, D.E., Clynne, M.A., Lowenstern, J.B., Sarna-Wojcicki, A.M., and Wooden, J.L., 2004, Age of the Rockland tephra, western USA: Quaternary Research, v. 62, p. 94–104.

Lipman, P.W., 1997, Subsidence of ash-flow calderas; relation to caldera size and magma-chamber geometry: Bulletin of Volcanology, v. 59, p. 198–218.

MacLeod, N.S., and Sherrod, D.R., 1988, Geologic evidence for a magma chamber beneath Newberry Volcano, Oregon: Journal of Geophysical Research, v. 93, p. 10067–10079.

MacLeod, N.S., Sherrod, D.R., Chitwood, L.A., and Jensen, R.A., 1995, Geologic map of Newberry Volcano, Deschutes, Klamath, and Lake Counties, Oregon: U.S. Geological Survey Miscellaneous Investigations Series I-2455, 23 p., 2 plates, scales 1:24,000, 1:62,500.

Mullineaux, D.R., 1974, Pumice and other pyroclastic deposits in Mount Rainier National Park, Washington: U.S. Geological Survey Bulletin 1326, 83 p.

Mullineaux, D.R., 1996, Pre-1980 tephra-fall deposits erupted from Mount St. Helens, Washington: U.S. Geological Survey Professional Paper 1563, 99 p.

Myers, B., and Driedger, C., 2008, Eruptions in the Cascade Range during the past 4,000 years: U.S. Geological Survey General Information Product 63, 1 sheet [http://pubs.usgs.gov/gip/63/].

Nathenson, M., 2001, Probabilities of volcanic eruptions and application to the recent history of Medicine Lake Volcano, *in* Vecchia, A.V., comp., A unified approach to probabilistic risk assessments for earthquakes, floods, landslides, and volcanoes, November 16–17, 1999, Golden, Colorado: U.S. Geological Survey Open-File Report 01-324, p. 71–74.

Nathenson, M., Thompson, J.M., and White, L.D., 2003, Slightly thermal springs and non-thermal springs at Mount Shasta, California; chemistry and recharge elevations: Journal of Volcanology and Geothermal Research, v. 121, p. 137–153.

Nathenson, M., Donnelly-Nolan, J.M., Champion, D.E., and Lowenstern, J.B., 2007, Chronology of postglacial eruptive activity and calculation of eruption probabilities for Medicine Lake volcano, northern California: U.S. Geological Survey Scientific Investigations Report 2007-5174-B, 10 p. [http://pubs.usgs.gov/sir/2007/5174/b/].

Poletski, S.J., 2010, The Nomlaki tuff eruption; chemical correlation of a widespread Pliocene stratigraphic marker: California State University Sacramento, Masters thesis, 96 p. [http://csus-dspace.calstate.edu/xmlui/handle/10211.9/210, accessed April 6, 2011].

Robinson, J.E., and Clynne, M.A., 2012, Lahar hazard zones for eruption-generated lahars in the Lassen Volcanic Center, California: U.S. Geological Survey Scientific Investigations Report 2012–5716–C, 13 p. [http://pubs.usgs.gov/sir/2012/5716/c/].

Sarna-Wojcicki, A.M., Meyer, C.E., Bowman, H.R., Hall, N.T., Russell, P.C., Woodward, M.J., and Slate, J.L., 1985, Correlation of the Rockland ash bed, a 400,000-year-old stratigraphic marker in northern California and western Nevada, and implications for middle Pleistocene paleogeography of central California: Quaternary Research, v. 23, p. 236–257.

Scott, W.E., Iverson, R.M., Vallance, J.W., and Hildreth, W., 1995, Volcano hazards in the Mount Adams region, Washington: U.S. Geological Survey Open-File Report 95-492, 11 p., 2 plates, scales 1:500,000, 1:100,000.

Sherrod, D.R., Taylor, E.M., Ferns, M.L., Scott, W.E., Conrey, R.M., and Smith, G.A., 2004, Geologic map of the Bend 30-X 60-minute quadrangle, central Oregon: U.S. Geological Survey Geologic Investigations Series I-2683, 48 p., 2 plates, scale 1:100,000.

Tabor, R.W., and Crowder, D.F., 1969, On batholiths and volcanoes—intrusion and eruption of late Cenozoic magmas in the Glacier Peak area, North Cascades, Washington: U.S. Geological Survey Professional Paper 604, 67 p., 1 plate, scale 1:62,500.

Tabor, R.W., Booth, D.B., Vance, J.A., and Ford, A.B., 2002, Geologic map of the Sauk River 30- by 60-minute quadrangle, Washington: U.S. Geological Survey Geologic Investigations Series I-2592, 67 p., 2 plates, scale 1:100,000.

Yamaguchi, D.K., and Hoblitt, R.P., 1995, Tree-ring dating of pre-1980 volcanic flowage deposits at Mount St. Helens, Washington: Geological Society of America Bulletin, v. 107, p. 1077–1093.

Produced in the Menlo Park Publishing Service Center, California
Manuscript approved for publication, August 17, 2012
Edited by Peter H. Stauffer
Layout and Design by Jeanne S. DiLeo